Title:

Temporal cohort number, neural composition, and connectivity vary along the *Drosophila* larval body axis

Authors:

Deeptha Vasudevan (1)

Yi-wen Wang (1)

Eliane Kushkowski (1-2)

Sean Corcoran (1-2)

Chris C Wreden (1-2)

Ellie S Heckscher (1-3)

Author Affiliations:

The University of Chicago, Chicago IL 60637

1) Department of Molecular Genetics and Cell Biology
2) Committee on Development, Regeneration and Stem Cell Biology
3) Institute for Neuroscience

Abstract (250 words)

Neural circuits are the fundamental computational units of the nervous system, and neural stem cell lineages are the fundamental developmental units of the nervous system. How these units map onto each other is a critical constraint on CNS function. The developing Drosophila nerve cord has emerged as a powerful model for studying lineage-based circuit assembly. Here, lineages are organized into temporal cohorts, which are sets of similar neurons born within a tight time window, and connectomic analysis shows that neurons of a temporal cohort have similar circuit-level connectivity. A major limitation has been the focus on a single representative segment, which is problematic because the body and nervous system comprise multiple segments organized into axially diverse regions, each with distinctive behaviors and circuits. How variation in stem cell lineage development impacts circuit configuration is unknown. Here, using the Drosophila NB3-3 lineage at different axial levels as a model, we determine the variation in cell biological decisions made by the lineage and examine its impact on temporal cohorts. We combined lineage tracing, manipulation of cell death pathways, marker gene analysis, and anterograde circuit tracing from somatosensory neurons. Depending on region, temporal cohort number is modulated by stem cell proliferation. The number and molecular identities of neurons within a temporal cohort are tuned by various cell biological mechanisms, all acting post-mitotically. Temporal cohorts can be mapped into similar or different circuits. Overall, this study provides new fundamental insight into how diverse circuits emerge from a constrained pool of stem cells in vivo.

Introduction

Neural stem cells have the potential to produce a dizzying array of neuron types in many different proportions and birth orders. The stem cell's decisions about which neurons to make, how many, and when they are created play profound roles in circuit wiring (Meng and Heckscher 2021). The process must be highly flexible: For example, sexually dimorphic circuits arise from the same stem cell pool in different organisms of a species. In evolution, homologous stem cell pools have generated organism-specific circuits. In vitro, researchers can differentiate stem cells along different trajectories to make various organoids. Despite the potential for flexibility, in vivo, the mapping of stem cell progeny into specific neuronal circuits must be exquisitely stereotyped and robust because when the process goes awry, the results include microcephalies, tumors, neurodevelopment disorders, and lethality. Despite its importance, we possess only a nascent understanding of the patterns in which neural stem progeny map to neural circuits.

In the past decade, some advances have been made in understanding stem cell-to-circuit relationships. Fundamentally, three stem cell-to-circuit patterns have been described: In "temporal matching," early-born neurons from one lineage wire with early-born neurons from a second lineage (Wang et al. 2022). In "sibling matching," sibling neurons from one lineage are connected (Wang et al. 2022). In "sequential assembly," output neurons of a circuit are born before their input neurons (Wang et al. 2022). Generally, a shared aspect of these wiring patterns is they are assembled from small sets (~5-6) of neurons born from a single stem cell within a tight time window, or "temporal cohorts." The discovery of temporal cohorts was seeded by an observation from an enhancer expression screen in Drosophila larvae (Manning et al. 2012): The larval NB3-3 stem cell lineage produces Even-skipped (Eve)-expressing Lateral (EL) neurons (Bossing et al. 1996). Halfway through development, the enhancer "11F02" is expressed in the NB3-3 stem cell and the ELs it produces, thereby subdividing EL neurons into early-born and late-born temporal cohorts (Wreden et al. 2017). Whole animal imaging and optogenetics showed early-born ELs process mechanical stimuli and can trigger escape-rolling, whereas late-born ELs process proprioceptive stimuli and regulate body posture (Wreden et al. 2017). When synaptic inputs onto early-born and late-born ELs in a single segment were identified using connectomics, this revealed statistically significant *similarities* in connectivity for early-born ELs and separately for late-born ELs and statistically significant *differences* between early-born and late-born ELs (Wang et al. 2022) (Fig 1C). These differences in wiring correspond to two NB3-3 temporal cohorts and show temporal cohorts are developmental units relevant to circuit wiring. Since their initial description in the NB3-3 lineage of the Drosophila nerve cord, many other temporal have been identified in this system (Meng et al. 2019)(Meng et al. 2020)(Wang et al. 2022). Temporal cohorts are also likely found in the adult Drosophila nerve cord (Baek and Mann 2009), mushroom body (Kunz et al. 2012), and vertebrate spinal cord (Stam et al. 2012), demonstrating the fundamental nature of temporal cohorts as a developmental unit across CNS circuits and phyla. However, there is still much to learn about temporal cohorts: One particularly significant gap in our understanding of temporal cohort biology is that analysis has focused on the level of the whole animal (Wreden et al. 2017) or a single "representative" segment (Meng et al. 2019)(Mark et al. 2021)(Meng et al. 2020)(Wang et

al. 2022), so we have no understanding of potential diversity in temporal cohorts. However, there is reason to believe there should be axial diversity in the circuits to which ELs and other temporal cohorts contribute.

In both vertebrates and insects, axially specialized motor circuits develop from segmentally repeating (or serially homologous) pools of stem cells. For example, in vertebrates, progenitors are organized into dorsal-ventral domains, such as p0, p1, p2, pMN, and p3 (Goulding and Lamar 2000) that are found along the entire developing neuroaxis axis, from the rostral hindbrain through the caudal spinal cord (Francius et al. 2013). In insects, a pool of ~30 types of neural stem cells (or neuroblasts Fig 1Ai) is found repeatedly from the anterior subesophageal zone (SEZ), a hindbrain-like region, through the posterior nerve cord (Figure 1Aii) (O Birkholz et al. 2013)(Technau et al. 2014)(Kunz et al. 2012). The need for axially specialized motor circuitry is evident from observing the body form of animals with prominent appendages at different axial levels, like humans, mice, and adult Drosophila, because appendages must be moved in a distinctive manner, which requires circuitry adapted for each movement type. Studies of central pattern-generating circuits reveal axial specialized CPGs in organisms as diverse as rats, chicks, turtles, lamprey, and leeches (Kjaerulff and Kiehn 1996)(Cohen 1987)(Ho and O'Donovan 1993)(Stein 2018)(Weeks 1982), showing that axially diverse motor circuits are fundamental.

Drosophila larvae possess a simple segmented tubular body (Fig 1B), making the need for diverse motor circuits less obvious. Nonetheless, the evidence for axial diversity is abundant: The larval body and CNS comprise four major regions, each consisting of multiple segments: SEZ, thorax, abdomen, and terminus. Studies of Drosophila larval CPG circuits demonstrate that the posterior-most abdominal segments have distinctive oscillations compared to more anterior segments of the abdomen and thorax (Pulver et al. 2015). Different regions of the Drosophila larval body have distinctive motor neurons and musculature (Dixit, Vijayraghavan, and Bate 2008)(Bate 1990)(Hartenstein 1993). Patterns of movement are regionally specialized (Dixit, Vijayraghavan, and Bate 2008)(Heckscher, Lockery, and Doe 2012). Manipulation of some Hox genes is sufficient to alter movement patterns (Dixit, Vijayraghavan, and Bate 2008). Still, manipulation of Hox genes in muscle alone cannot transform movement, demonstrating that differences in CNS circuits underlie specialized movements (Dixit, Vijayraghavan, and Bate 2008). In addition to differences in motor output, there is likely specialization in somatosensory processing circuitry because the number of somatosensory neurons in the periphery varies by body region (Bodmer and Jan 1987)(Fig 1B). So, it is also likely that axial differences exist in central circuits that process larval somatosensory stimuli.

From a developmental perspective, there is strong evidence for axial diversity in neural development starting from a highly constrained pool of stem cells. Embryological "cut and paste" experiments in chicks moved progenitors from developing wing levels to developing hindlimb levels and vice versa, generating chickens that move their legs synchronously, similar to wing beats and wings moving with left-right alternation similar to walking (Narayanan and Hamburger 1971). Thus, although progenitors appear similar at the cellular level, they possess the intrinsic ability to generate axially diverse circuitries. Previous studies have shown that in the developing CNS, Hox genes regulate the axial diversity of neural stem cell proliferation (Bahrampour, Jonsson, and Thor 2019)(Monedero Cobeta, Salmani, and Thor 2017)(Gouti and Gavalas 2008)(Seifert 2015)(Homem, Repic, and Knoblich 2015)(Tsuji, Hasegawa, and Isshiki

2008)(Berger et al. 2005), motor neuron identity (Jungbluth, Bell, and Lumsden 1999)(Hobert 2021)(Jung et al. 2010)(Dasen and Jessell 2009)(Dasen et al. 2005)(Kessel 1994), and neurotransmitter type (Feng et al. 2022)(Lints and Emmons 1999)(Estacio-Gómez and Díaz-Benjumea 2014)(Suska, Miguel-Aliaga, and Thor 2011)(Feng et al. 2020). Most of these studies seek to uncover the molecular mechanisms involved in directing specific cell biological processes, emphasizing the production of neural diversity. One consequence is that for any given lineage, knowledge about what cell biological processes occur in which region is fragmentary; second, it is unknown how the axial diversity of cell biological mechanisms might diversify temporal cohorts and impact circuit configuration.

To understand how cell biological variations in serial homologous neural stem cell lineage development specialize temporal cohorts, we use NB3-3 neuroblasts (Fig 1A) and their Even-skipped Lateral (EL) neural progeny as a model (Figure 1C-F). We combined lineage tracing, manipulation of cell death pathways, marker gene analysis, and anterograde circuit tracing from somatosensory neurons. Our data support the following model: Depending on the region, temporal cohort number is modulated by stem cell proliferation (Fig 1Fi). The number and molecular identities of neurons within a temporal cohort are tuned by various cell biological mechanisms, acting post-mitotically (Fig 1Fii). Temporal cohorts can be mapped into similar or different circuits (Fig 1Fiii). This provides a new framework for understanding how cell biological variation in stem cell lineage development impacts circuit configuration.

Methods

Drosophila Strains and Culture

Fly stocks were maintained at 25°C on a standard cornmeal molasses medium. Experimental crosses were set up at the indicated temperatures. The following fly lines were used:

Name	Genotype	Location	Source
Wild type	*w1118*	x	Heckscher, et al 2015(Marshall and Heckscher 2022) (Heckscher et al. 2015)
H99	*Df(3L)H99*	3	BL #1576
p35	*UAS-p35*	2	BL #5072
Elav-GAL4	*Elav-GAL4*	X	BL #5144
G-TRACE	*P{w[+mC]=UAS-RedStinger}4, P{w[+mC]=UAS-FLP.D}JD1, P{w[+mC]=Ubi-p63E(FRT.STOP)Stinger}9F6*	2	Evans et al., 2009; BL #28280
EL-GAL4	*EL-GAL4*	3	Heckscher et al., 2015
Twin Spot MARCM	*UAS-rCD2.RFP.UAS-GFPi/CyO; TM3/TM6B*	2	BL #56184
Twin Spot MARCM	*UAS-mCD8.GFP.UAS-rCD2i/CyO; TM3/TM6B*	2	BL #56185
11F02-GAL4	*P{R11F02-Gal4 (w+)}attP2*	3	BL#49828
UAS-nls-GFP	*P{UAS-GFP::lacZ.nls}30.1, (w+)*	3	BL# 6452
TransTango	*y[1] w[*] P{y[+t7.7] w[+mC]=UAS-myrGFP.QUAS-mtdTomato-3xHA}su(Hw)attP8; P{y[+t7.7] w[+mC]=trans-Tango}attP40*	1,2	Talay et al., 2017; BL# 77124
IAV-GAL4	*IAV-GAL4*	2	BL#36360
0165-GAL4	*0165-GAL4*	3	Marshall et al., 2022

Embryos and early-stage larvae were used. At these developmental stages, flies have no distinguishing sexual characteristics. Thus, all experiments were conducted in a manner that was blind to sex.

Tissue preparation

Four tissue preparations were used: (1) Late-stage whole mount embryos, in which antibodies can still penetrate the cuticle; (2) late-stage dissected embryos, in which the neuromuscular tissue and cuticle are dissected away from the CNS, allowing for superb immuno-labeling and visualization of the entire axial nerve cord from SEZ to terminus; (3) isolated larval CNSs, in which the CNS is removed from other larval tissue so that antibodies reach the CNS's. For all

preparations, standard methods were used for fixation in fresh 3.7% formaldehyde (Sigma-Aldrich, St. Louis, MO). Embryos were staged for imaging based on standard morphologic criteria.

Immunohistochemistry

Tissue was washed three times with phosphate-buffered saline containing 0.1% Triton X-100 (PBT), blocked 1 hr in PBT containing 2% normal goat serum (NBT), and stained with primary antibody in PBT at 4°C overnight. After washing, samples were stained with secondary antibody at room temperature for 1 hr, washed again, and applied with increasing percentages of ethanol in water (30, 50, 70, 95, 100) series to replace PBT. Samples were then immersed into xylene for clearance and mounted in DPX (Sigma, MI). Images were acquired using a Zeiss LSM 800 confocal microscope and processed and analyzed using ImageJ. The following primary antisera were used:

Antibody	Species	Dilution factor	Source
anti-Eve	rabbit	1:1000	Meng, et al., 2019
anti-GFP	guinea pig	1:2000	Rick Fehon, UChicago
anti-mCherry	chicken	1:1000	Novus NBP2-25158
anti-Hey	guinea pig	1:1000	Delidikis, University of Crete

Secondary antibodies were obtained from ImmunoResearch (Bar Harbor, ME) and were used at a 1:400 dilution.

Imaging, Statistics, Figure assembly

Images were acquired on a Zeiss 800 confocal microscope with 40× objective. Test and descriptive statistical analyses were performed using Prism (GraphPad). Figures were assembled using Fiji and Adobe Illustrator.

Cell counts

This procedure is for counting cells in a z stack, particularly cells in a cluster that are challenging to count by eye. Using the Multi-point tool in FIJI, it is possible to label each cell with a numbered point to show the presence of all cells in a cluster. This works well for images taken at 2048 x 2048 with approx. 0.5 micron slices. (1) Open .czi file in FIJI and select the channel of interest. (2) Go to Process/Enhance Contrast... and change Saturated Pixels to 0.1%. Select Normalize and Process all slices before pressing OK. (3) Go to Process/Noise/Despeckle to further process the image before analysis. (4) Save the changes as a .tif. (5) Open the .tif, scroll to the first slice where a cell appears, and zoom in on the cell cluster. Use the + and - keys to zoom to avoid moving points erroneously. (6) Select Multi-point in the FIJI toolbar and double-click to open the Point tool window. Set Type to Hybrid, Size to Tiny, and select Label points. Set counter to 1. Press OK. (7) With Multi-point tool selected, click on the center of a cell to drop a point. Scroll through the stack and drop point on each slice until the cell is no longer visible. With slices of approx. 0.5 microns cells should be present in 6-8 slices. (9) Return to the Point tool window and set counter to 2. Repeat to mark the remaining cells. (1) Notes specific to counting ELs: Label U neurons to ensure that Us are not counted as ELs, using the 0 counter to do this.

ts-MARCM experiments

We used an internal reference to precisely estimate when heat shocks were provided to the embryos to induce recombinase expression and initiate the lineage trace. This is because heat shocks were provided to embryos for 2-to 3-hour windows, it takes several hours for FLP to induce a genetic change (Wang et al. 2022), and neuroblasts divide every 45 minutes. This internal reference system works on the developmental principle that unlike vertebrates and long-germ band insects where axial development is temporal offset, with the anterior developing before the posterior, in short-germ band insects like *Drosophila* segments develop synchronously. So, it is reasonable to assume that neuroblasts are dividing at approximately the same time along the A-P axis, and there are no differences between left and right hemi-segments. We found that most CNS had multiple clones (Figure 5E). For each CNS, we assessed each clone's location and size. Because we know NB3-3 divides for the duration of embryogenesis (Gunnar et al. 2016), the number of EL labeled in the abdomen is directly related to the number of NB3-3 divisions yet to occur. If one or more clones were found within the abdomen, we used it to calculate the max abdominal clone size per CNS; using the max abdominal clone size serves as our internal reference. The maximum abdominal clone size is a proxy for the earliest an embryo could have been heat-shocked. We sorted each clone into bins based on its max abdominal clone size in its CNS. This binning generates the X-axis in Figure 5-H and is labeled as "heat shock relative to inferred NB3-3 division number".

Results

This study aimed to understand how cell biological variation in stem cell lineage development diversifies temporal cohorts. We studied EL temporal cohorts at different axial levels of the Drosophila larval CNS as a model. The Drosophila CNS develops from an initial base array of 30 molecularly distinct types of stem cells (neuroblasts)(C Q Doe 1992). Each left or right hemisegment possesses one of each type of neuroblast, and this pattern is repeated in segments from head to tail, meaning neuroblasts are serially homologous (Fig 1A). For example, the NB3-3 stem cell is found in 14 segments from SEZ2 to Te2. In the first abdominal segment, the NB3-3 produces two temporal cohorts of ELs—early-born and late-born— mapped into different somatosensory processing circuits (Fig 1C). However, in the thorax, NB3-3 neuroblasts never produce late-born ELs (Heckscher et al. 2014)(Tsuji, Hasegawa, and Isshiki 2008). This indicates that in different axial regions, serially homologous stem cells produce different numbers of temporal cohorts and raises the question of how general this occurrence is and what additional features of variation are. To address these questions, we characterized four axial regions of the larval CNS. From the anterior, they are the SEZ (comprised of 3 segments), thorax (3 segments), abdomen (7 segments), and terminus (2 segments) (Fig 1A-B). For the NB3-3 lineage in each segment, we monitored proliferation, cell death, differentiation, identity, and circuit membership. Our data link cell biological decisions to the specialization of temporal cohorts and associate it with circuit wiring outcomes. This helps us understand the in vivo developmental flexibility in patterns of neural stem progeny that map to neural circuits.

NB3-3 produces different numbers of Even-skipped (Eve) Lateral neurons in different segments along the body axis.

In all organisms, the number of somatosensory neurons varies along the body axis. Theoretically, the number and/or connectivity of sensory processing neurons in the CNS should also vary along the body axis to accommodate differences in incoming somatosensory stimuli. In Drosophila larvae, the abdomen has 43 left-right mirror image sets of somatosensory sensory neurons, found repeatedly in every segment A1-A7, with fewer in the thorax and terminus (Bodmer and Jan 1987)(Fig 1B). ELs are all somatosensory neurons because they require sensory input to fire (Heckscher et al. 2015). So, to what extent do ELs vary along the body axis?

To determine how ELs vary in <u>number</u> within the nerve cord, we counted ELs in the larval CNS after ELs were already incorporated into functional circuits (Fig 1D-E). Consistent with prior reports, there are half the number of ELs in the thorax compared to the abdomen (Heckscher et al. 2014). We found that the terminus possesses four ELs, three in Te1 and one in Te2 (Fig 1D-E). Thus, the distribution of EL number generally mirrors that of somatosensory neurons—more in the abdomen, fewer in the thorax and terminus. Notably, we found an additional EL in segments A2-A7 compared to A1. In A1 versus A2-A7, the number of somatosensory neurons is identical, so differences in EL numbers were unexpected. Therefore, we repeated counts of A1 and A2 specifically, using higher resolution airy scan confocal microscopy, confirming the unexpected numerical difference (Figure S1). The physiological reason for this additional EL in A2-A7 is unknown.

NB3-3 neuroblasts are present in the hindbrain-like SEZ (O Birkholz et al. 2013). The SEZ does not get input from body wall somatosensory neurons, so we had no prior expectations about EL numbers in this region. We newly found that in segments SEZ2-3, ELs form four clusters of ~5-6 neurons each, which could correspond to two temporal cohorts (Figure S2). Numerically, the number of ELs in SEZ is similar to the abdomen, which possesses two temporal cohorts, and is different from the thorax, which possesses only one EL temporal cohort.

Our data show that NB3-3 stem cells produce different numbers of EL in various regions of the developing Drosophila CNS, making this an excellent model for studying how variation in the development of stem cell lineages diversifies temporal cohorts.

Programmed cell death of EL neurons partially limits their number in terminal segments.

In the CNS of mice, *C. elegans*, and Drosophila, ~50% of embryonically born neurons die during normal development. In flies and mice, neural cell death is essential for viability (Fuchs and Steller 2011)(Ellis 1986)(Fricker et al. 2018)(Yamaguchi and Miura 2015)(Kuan et al. 2000), making cell death an obvious candidate for regulating EL number in various segments along the body axis. Programmed cell death has been observed in the NB3-3 in the terminus (Oliver Birkholz et al. 2013). However, it remains unknown if ELs die, if NB3-3 dies, and the extent to which there is cell death in lineage outside the terminus.

To determine if terminal ELs die, first, we counted EL numbers in segments A7, Te1, and Te2, starting at stage 13, just after early-born ELs are born (Tsuji, Hasegawa, and Isshiki 2008) and ending at larval stages after all ELs are generated. Within this period, EL numbers doubled in A7 but decreased in both segments of the terminus (Fig 2B-C), demonstrating EL number is regulated differently in the terminus relative to the abdomen. Still, we could not conclude that the reduction was due to cell death or another mechanism (e.g., failure to express *eve*).

To determine the role of programmed cell death (PCD) in ELs, we blocked PCD specifically in neurons. Using the pan neural driver, ElaV, we drove the p35 Caspase inhibitor. EL number is unchanged in A7 and more anterior segments (Fig 2D-F) but increases in the terminus from 3 to 5 in Te1 and in Te2 from 1 to 2 (Figure 2A, D-F). Thus, ~50% of EL neurons in the terminus are pruned by programmed cell death after birth.

When blocking neural cell death, the EL number in the terminus does not recover to abdominal levels (~11-12), suggesting additional limits on the EL number in the terminus. To test if these limits were imposed by the death of the NB3-3 stem cell in the terminus, we used *Df(3L)H99* mutants to block <u>both</u> neuroblast and neuronal programmed cell death. In the mutants, EL numbers return to ~5 in Te1 and ~2 in Te2 (Figure 2A), similar to the neural-specific block in cell death. We have no evidence that the EL number in the terminus recovers to the levels seen in the abdomen.

We conclude that neuronal programmed cell death is a major regulator of EL number, and it is selective for the terminus (Fig 2D). Neither cell death of neurons nor stem cells can explain why EL counts in the terminus fail to reach abdominal levels (~12) because they remain closer to thoracic numbers (~5). This suggests that additional mechanisms beyond cell death must limit EL numbers in the terminus.

In A1 and the terminus, Eve is not expressed in all neurons of the NB3-3B hemilineage

Even-skipped is an evolutionarily conserved homeodomain transcription factor expressed in small subsets of neurons in animal CNS tissue across phyla (Heckscher et al. 2015). In mice, flies, and *C. Elegans*, Eve homologs regulate neural identity and axon pathfinding (Ahringer 1996)(Fujioka et al. 2003) (Moran-Rivard et al. 2001). In Drosophila larval ELs, Eve is also required for normal movement, somatosensory stimulus encoding, and dendrite morphology (Marshall and Heckscher 2022). Thus, whether or not to express *EVE* is a critical decision for a cell and is likely to be highly regulated. To what extent is the EL number at different axial levels regulated at the level of *eve* expression? Specifically, to what extent are there neurons that might be expected to express eve but fail to do so?

In Drosophila, each neuroblast can make two hemilineages—A and B (Fig 3A) that dramatically differ based on Notch signaling (e.g., in morphology and neurotransmitter expression). Neurons of a hemilineage usually share transcription factor expression patterns with neurons of the NB3-3B hemlineage generally expressing *eve* (Lacin et al. 2019). However, we recently found that in segment A1, the first-born NB3-3B neuron is undifferentiated and fails to express *eve* (Wang et al. 2022), raising the possibility that NB3-3B neurons in other segments may similarly fail to express *eve,* and this could limit EL number.

We evaluated *eve* expression in NB3-3B neurons using lineage tracing to permanently mark NB3-3 and its progeny with a nuclear-localized GFP (Fig 3A). We expressed nuclear-localized GFP in *Eagle-GAL4*-expressing cells and their descendants using the GAL4 Technique for Real-time And Clonal Expression (G-TRACE) (Evans et al. 2009). *Eagle-GAL4* is expressed in four types of neuroblasts and a subset of their progeny (Higashijima et al. 1996). The NB3-3 lineage can be identified among the four labeled lineages based on position in all segments except SEZ2 (Fig 3Bi). Within the NB3-3 lineage (GFP+ cells, Fig 3Ai), labeling with the pan-neural marker (anti-ElaV Fig 3Bii) and the neural Notch reporter (anti-Hey Fig 3Biii) distinguishes NB3-3 neuroblasts, NB3-3A neurons, and NB3-3B neurons (Figure 3A-B). Co-labeling with anti-Eve (Fig 3Biv) reveals how many NB3-3B neurons fail to express *eve*.

To calibrate this approach, we counted the number of Eve(-) NB3-3B neurons in A1, finding that in half of our observations, one NB3-3B neuron fails to express Eve (Fig 3C, E). Applying this metric to other segments shows that all NB3-3B neurons in A2-A7, thorax, and SEZ are Eve(+) (i.e., none fail to label with anit-Eve Figure 3C, E). In contrast, in both terminal segments, Te1 and Te2, a subset of NB3-3B neurons, fail to express Eve (Figure 3Bv-ix, C, E).

We conclude that an additional mechanism to regulate EL number is the regulation of *eve* expression. Like PCD, this mechanism is prominent in the terminus, but in this case, it is not exclusive to the terminus. Together, PCD and *eve* regulation cannot account for the smaller number of ELs in the terminus compared to the abdomen, strongly suggesting that the remaining difference in EL number can only be accounted for by differences in proliferation.

Proliferation patterns of NB3-3 vary along the body axis to produce different numbers of temporal cohorts in various regions.

The CNS is particularly sensitive to defects in cell division and requires specific proliferation control mechanisms (Homem, Repic, and Knoblich 2015). Two prominent models for studying neural proliferation are mammalian cortical progenitors and Drosophila neural stem cells. Extensive work in these systems has described division patterns, molecular mechanisms ensuring proliferation control, and the defects that can occur when proliferation control is disrupted. Far less is known about specific physiological contexts in which proliferation impacts circuit configuration.

Having found that post-mitotic mechanisms are only partially responsible for regulating EL number (Fig 2-3), we evaluated the role of proliferation as a determinant of EL number. NB3-3 neuroblast proliferation patterns differ between the thorax and abdomen: In the abdomen (Figure 4C), NB3-3 neuroblasts produce a ganglion mother cell (GMC) in its first division, which divides to produce two neurons with distinct binary cell fates, and after that, NB3-3 neuroblasts divide to produce neurons directly (Gunnar et al. 2016). Abdominal NB3-3 neuroblasts divide for the duration of embryonic neurogenesis to produce both early-born and late-born ELs (Tsuji, Hasegawa, and Isshiki 2008)(Wreden et al. 2017)(Wang et al. 2022). In contrast, in the thorax (Figure 4B), NB3-3 neuroblasts repeatedly produce GMCs until halfway through embryonic neurogenesis, when the neuroblasts enter quiescence (Gunnar et al. 2016)(Tsuji, Hasegawa, and Isshiki 2008). The effect is that thoracic NB3-3 neuroblasts produce only the early-born temporal cohort. These observations raise the possibility that NB3-3 proliferates in a bimodal manner, producing either the early-born temporal cohort or both early-born and late-born temporal cohorts. We tested this possibility by examining neurogenesis in the SEZ and terminus.

To analyze the NB3-3 division, we used an inducible lineage tracing approach, Twin-spot mosaic analysis with a repressible cell marker (ts-MARCM) (Yu et al. 2009). Heat shocks can be applied at various developmental time points to induce the lineage trace (e.g., Fig 4C-E), delivering recombinase to random cell sets. If recombination occurs in a dividing cell, the cell's progeny can be genetically altered. GFP can label one daughter and all its descendants, and RFP can label the other daughter and all its descendants. Because GFP and RFP are under UAS- control, they are only detected in cells expressing GAL4.

We mined a ts-MARCM dataset that was previously produced by Wang (Wang et al. 2022) that had been used to birth date each EL in segment A1. Recombination events were detected using *EL-GAL4*, which labels all EL neurons. The Wang 2022 dataset includes ~12 different heat shock protocols, 80 CNS, and 234 clones (Table 4-S1). Herein, "clone" refers to a group of cells labeled by one recombination event. Approximately half the CNSs were imaged at low resolution for all regions (SEZ to terminus), and the remainder were imaged at higher resolution for nerve cords only (thorax to terminus). Generally, clones were found along the entire axis, with clones in multiple segments in each CNS (Fig 4E-E', Table 4-S2). We binned each CNS based on heat shock time relative to the inferred NB3-3 division number, where 1 represents the first neuroblast division, and 11 represents the last division (see methods for details) (Fig 4F-H). For the present study, the Wang dataset provides three new types of information: 1) <u>When NB3-3 is dividing (e.g., Fig 4G).</u> Recombinase will not generate a clone if the lineage trace is induced after the neuroblast completes division. 2) <u>What cell type is dividing (e.g., Fig 4H).</u> If recombination occurs in a GMC, the clone will comprise at most two neurons

regardless of induction time. Herein, only one of the two is detected by *EL-GAL4*. But, if recombination occurs in a dividing neuroblast, it will produce a large clone because all of its progeny will be labeled, and recombination events induced earlier in development label more progeny. 3) If the EL is differentiated (e.g., Fig 4I-J). Differentiated neurons have a soma size of >3 microns (Heckscher et al. 2014), and undifferentiated neurons are smaller (~1.5 microns).

First, we analyzed the abdomen to relate ts-MARCM data to previously published reports. In the abdomen, clones were generated at all induction times (Fig 4F-G), indicative of abdominal NB3-3 dividing for the duration of embryogenesis. Among all abdominal clones, the percentage of small clones (e.g., 1:0 or a singly labeled EL) at each induction time was in the minority (Fig 4F, H), indicative of the rarity of GMC division in the abdomen (Gunnar et al. 2016). Interestingly, in 80% of CNS in which EL in A1 and A2-A7 were labeled, the number of ELs in A1 was fewer than other abdominal segments (Table 4-S2), consistent with the idea that the first division of NB3-3 produces an Eve(+) in A2-A7, but not in A1 (in agreement with Fig 3E).

In the thorax, clones are robustly generated by early but not late ts-MARCM induction (Fig 4G), indicative of NB3-3 entering quiescence midway through neurogenesis (Tsuji, Hasegawa, and Isshiki 2008). At nearly all induction times, clones were small (Fig 4H), indicating that while NB3-3 is dividing, it produces GMCs. Newly, we found the thorax, but no other regions, possess EL with small soma (Fig 4I-J). So, a subset of thoracic ELs expresses Eve but does not differentiate (Fig 4I).

In the SEZ, NB3-3 appears to divide continuously for embryonic neurogenesis. The SEZ-containing dataset is skewed toward later ts-MARCM inductions (from the inferred 5th division of NB3-3 onwards, Table 4-S2). Within the dataset, ELs are labeled regardless of induction time, and robust SEZ clonal production at late induction times produces abdominal clones but not thoracic clones (Fig 4G). Most SEZ clones comprise single-labeled ELs regardless of induction time (Fig 4H), suggesting that dividing GMCs are present throughout embryogenesis.

The ts-MARCM dataset had only a few clones in the terminus, likely because there are so few ELs in that region. Like the thorax, terminal clones were generated by early but not late heat shocks (Fig 4G), consistent with the idea that NB3-3 stops divining mid-embryogenesis in the terminus. Previously, Birkholz speculated that NB3-3 neuroblasts in the terminus may go into quiescence as they do in the thorax (Oliver Birkholz et al. 2013). Our ts-MARCM data and the cell death data in Figure 2 support this speculation. Birkholz also suggested that other aspects of the NB3-3 division pattern (presence of GMCs) would be thoracic-like (Oliver Birkholz et al. 2013). However, Gunnar speculated that terminal NB3-3 neuroblasts should behave like abdominal neuroblasts (Gunnar et al. 2016). We needed a second method to assay the division pattern because there were so few ts-MARCM clones in the terminus.

As an independent assessment of the division patterns in each region, we counted neurons in the NB3-3A hemilineage, which are only produced if NB3-3 is present and undergoing a type 1 division pattern (i.e., with a GMC). Generally, our findings match published reports and validate our conclusions based on ts-MARCM data: Each abdominal segment has a single Hey(+) NB3-3A neuron. The number of NB3-3A neurons matches the EL number for each thoracic and SEZ segment. We also learned that each terminal segment possesses a single NB3-3A neuron, which agrees with the Gunnar model (Gunnar et al. 2016).

We conclude that in each of the four major regions—SEZ, thorax, abdomen, and terminus, NB3-3 has a distinctive proliferation pattern (Fig 4A-D). Generally, we conclude that an early-born EL temporal cohort is produced in all segments. NB3-3 neuroblasts stop dividing midway through neurogenesis in the thorax and terminus before producing the late-born cohort. However, in the SEZ and abdomen, NB3-3 neuroblasts proliferate for embryonic neurogenesis, generating both early-born and late-born temporal cohorts of EL neurons. Notably, there are slight differences in proliferation among regions, with, for example, NB3-3 in Th3 dividing six times compared to five in other thoracic segments. This raises the question of whether there are additional ways in which temporal cohorts may be regionally specialized.

Regardless of region, early-born and late-born ELs express similar identity markers.

Enormous cell diversity is a hallmark of nervous systems. Generally, single-cell transcriptional studies reveal correlations of well-defined transcriptomes with specific neuronal identities. Neuronal identities can be assayed by detecting the expression of transiently expressed transcription factors that sit atop genetic cascades. In Drosophila, neural identity differences are established by dynamic temporal transcription factor cascades in neural stem cells (Chris Q Doe 2017). So, examining neural identity markers reveals both neural diversity and can point to variation in temporal patterning mechanisms. In segment A1 of the abdomen, early-born ELs express Krupple and Knot (Tsuji, Hasegawa, and Isshiki 2008)(Demilly et al. 2011) and late-born ELs express the enhancer 11F02 (Wreden et al. 2017). 11F02 is an enhancer for the Pdm transcription factor. The question we address here is to what extent do temporal cohorts in different regions differ at the level of molecular identities?

First, we assayed the expression of the late-born marker 11F02. Abdominal ELs, A1-A7, express 11F02, but not thoracic ELs, Th1-3 (Fig 5A-B). These data confirm prior studies (Wreden et al. 2017)(Heckscher et al. 2014) and extend from exemplar (T2-A1) segments to the whole thorax and abdominal regions. The terminus lacks a late-born EL temporal cohort and 11F02 expression (Fig 5B). The SEZ possesses a late-born EL temporal cohort, and a subset of ELs in that region express 11F02. This suggests that late-born ELs produced in different regions have similar molecular identities.

Next, we assayed the expression of the early-born marker Kr (Tsuji, Hasegawa, and Isshiki 2008)(Wreden et al. 2017). All segments possess the early-born temporal cohort (Fig 4A). However, across segments, the number of Kr+ ELs significantly varies: Te2 possesses zero, Te1 possesses one, Th1-2 and A2-A7 possess two, whereas SEZ3, Th3, and A1 possess three (Figure 5C). The small number of Kr+ ELs in the terminus could be explained by programmed cell death in that region. However, available data cannot explain why two versus three Kr+ ELs exist in other segments. We investigated Kn expression to determine if other markers also varied in early-born temporal cohorts (Demilly et al. 2011). Segments SEZ3-A7 show a slight variance in Kn(+)EL number (Fig 5D), and ELs in Te1 and Te2 express Kn, confirming their early-born molecular identity is shared with ELs in other segments (Fig 5D).

We conclude that early-born and late-born ELs produced in different regions have similar molecular identities. However, at least some aspects of early-born ELs' specific molecular identities can vary between segments. We do not know the consequence of tuning molecular identities; it could involve anatomy, function, or both.

Early-born temporal cohorts can be mapped into similar and different circuits in different regions.

Temporal cohorts are important because they are fragments of lineages that act like developmental units mapped into specific circuits. For example, NB3-5 produces an early-born temporal cohort of RP motor neurons that innervate ventral muscles (Meng et al. 2020); NB7-1 produces an early-born temporal cohort of U motor neurons that innervate dorsal muscles (Meng et al. 2019). Like NB3-3, NB3-5, and NB7-1, neuroblasts are serial homologs along the body axis, found repeatedly from SEZ to the terminus. Yet, the body wall muscles vary significantly in number and arrangement in different regions (Hartenstein 1993), strongly suggesting that developmental mechanisms must specialize circuits that control body wall muscles, including regulating motor neuron number, and that this occurs downstream of stem cell production. For NB3-3, in segment A1, connectomics demonstrates direct synaptic connections between mechanosensitive chordotonal sensory neurons and each early-born EL and direct synaptic connections between proprioceptive sensory neurons and each late-born EL (Wang et al. 2022). The differences we found in molecular identity among ELs, at least within the early-born temporal cohort (Fig 5), hint at the possibility of differences in how temporal cohorts are mapped into circuits. Here, we ask what somatosensory processing circuits the EL of the nerve cord is mapped to.

We used anterograde tracing to identify somatosensory inputs onto ELs along the body axis. Specifically, we used Trans-tango, in which a GAL4 line labels the starting (GAL4-expressing) neurons in green and their downstream synaptic partners in red (Fig 6A-B). Here, we used either *IAV-GAL4* to identify downstream targets of mechanosensitive CHO somatosensory neurons or *0165-GAL4* to identify downstream targets of the proprioceptive dorsal bipolar dendrite (DBD) sensory neuron (Fig 6C). We additionally labeled the tissue with anti-Eve antibodies to determine the extent to which ELs in different segments and regions received input from either sensory neuron class (Fig 6A).

First, to validate Trans-tango for use in larval Drosophila, we examined segment A1 because we have connectivity data from the connectome for comparison (Wang et al. 2022). ELs in A1 were labeled as post-synaptic to both CHOs and DBD, as expected. We also co-stained with the early-born markers Kn in a small subset of samples. As expected, tracing from CHOs but not DBDs robustly labeled Kn+ ELs. When we used Trans-tango to evaluate connectivity for the remainder of the abdomen, A2-A7, we found evidence of direct synaptic inputs from CHOs and DBD (Fig 6D-E). This suggests that connectivity in A1 is representative of connectivity in other abdominal segments. CHOs but not DBD labeled ELs in the terminus, which is consistent with the observation that the terminus possesses early-born but not late-born ELs (Fig 6D-E). Unexpectedly, however, ELs in the thorax <u>were not</u> labeled by Trans-tango from either type of somatosensory neuron (Fig 6D-E).

Our results suggest that late-born ELs get input from proprioceptors when present in the abdomen. Further, early-born ELs in all abdominal and terminal segments get input from CHOs, showing that temporal cohorts in different regions can be mapped into similar circuits. However, early-born ELs in thoracic segments do not get input from CHOs, showing that temporal cohorts in the different areas can also be mapped into similar circuits. Although we did not examine ELs

in the SEZ, we expect the EL temporal cohorts in that region could be mapped to other circuits because the SEZ does not receive projections from body wall somatosensory neurons. We conclude there is complexity and flexibility mapping between temporal cohorts and circuits.

Discussion

In summary, our data show how variation in stem cell lineage development can impact the axial specialization of temporal cohorts. Our data support a three-part model. First, the temporal cohort number is modulated by the duration of stem cell proliferation—producing different temporal cohorts in various regions (Figure 4). Second, the number of neurons within a temporal cohort (Figure 1) and molecular identities (Figure 3) vary across segments and regions, and this is because once established, temporal cohorts are diversified by various cell biological mechanisms acting post-mitotically, including programmed cell death (Figure 2), regulation of gene expression (Figure 3), and neural differentiation status (Figure 4I-J). Finally, similar temporal cohorts in different regions can be mapped into similar or different circuits, depending on the region (Figure 6). We provide an understanding of how variation in developmental trajectories of stem cell lineages impacts circuit configuration.

Neuroblast proliferation duration determines the temporal cohort number.
When we started this project, we knew two EL temporal cohorts in A1, early-born and late-born, each consisting of 5 or 6 neurons (Wreden et al. 2017)(Wang et al. 2022). In the thorax, only 5 or 6 EL neurons were generated (Heckscher et al. 2014), and they were generated early in development (Tsuji, Hasegawa, and Isshiki 2008). So, we knew that between the thorax and the abdomen, NB3-3 switched modes, producing either one or two temporal cohorts. In theory, NB3-3 could produce any number of neurons, so we wondered if NB3-3 acted in a bimodal manner, or if the early-born / late-born switch was a coincidence observed only in the abdomen and thorax, and if there was a graded distribution in the number of EL neurons made by NB3-3 in segments of other regions.

We looked at other segments and found evidence for the bi-modal proliferation pattern of NB3-3. NB3-3 neuroblasts in SEZ produce 10-12 neurons (Figure 1) and early- and late-born temporal cohorts (Fig 4-5). NB3-3 neuroblasts in the terminus produce only the early-born temporal cohort (Fig 4-5). In Te1, NB3-3 neuroblasts generate ~5 Eve+ ELs (Figure 2) plus an additional NB3-3B neuron that fails to express Eve (Figure 3), and in Te2, NB3-3 neuroblasts generate ~2 Eve+ ELs (Figure 2) plus three additional NB3-3 neurons that fail to express Eve (Figure 3). Adding these numbers together, we learn that, in the terminus, NB3-3 neuroblasts generate 5 or 6 neurons, precisely as they do in the thorax.

Duplicating temporal cohorts might be a mechanism for the nervous system to introduce new functions. Much like the gene “duplicate and diverge” model, temporal cohorts could be duplicated units and then diverge over evolutionary time scales. Applying a duplicate and divergence idea to temporal cohorts is based on the idea that Th2 is the default state because when all Hox genes are mutant, other segments adopt Th2 fates (Lewis 1978). If Th2 is the default state, NB3-3 producing one early-born EL temporal cohort is the default state. In the SEZ and abdomen, NB3-3 neuroblasts would duplicate the early-born temporal cohort, creating a late-born temporal cohort of ELs, which diverged from the early-born temporal cohort as evidenced by differences in gene expression and connectivity patterns (Figure 5-6).

Post-mitotic mechanisms can tune neurons' number and molecular identities within a temporal cohort. Once the number of temporal cohorts is established, the neuron numbers and

their molecular identities can be tuned in some cases. For EL number, we find three distinctive cell biological mechanisms that are expressed in neurons that tune EL number—(1) regulation of Eve expression, (2) programmed cell death, and (3) differentiation status. Eve fails to turn on in neurons in adjacent (Te1 and Te2), and non-adjacent segments (A1)(Figure 3), showing this mechanism is axially distributed. Axial distribution implies that diverse Hox inputs (e.g., Ubx in segment A1 and Abd-B in the terminus) could converge at the level of regulation of *eve* expression. However, other cell biological mechanisms are specific to one region: cell death in the terminus (Figure 2) and failure to differentiate in the thorax (Figure 4I-J). In all cases, from a circuit perspective, the effect is to alter the number of neurons available for wiring. We currently do not know precisely why the number of ELs is reduced. Based on the programmed cell death literature (Kuan et al. 2000)(Yamaguchi and Miura 2015)(Fricker et al. 2018)(Fuchs and Steller 2011), there are three possibilities: (1) elimination of unused, functionally redundant neurons that lack targets, (2) elimination of defective cells, or (3) elimination of neurons that, if left undead, would incorporate into circuits to provide additional presumably unwanted functions.

An unexpected observation is that EL numbers are modulated in early-born EL temporal cohorts but not late-born temporal cohorts. A fundamental challenge for animals that develop from neural stem cells is that not all neurons, circuits, and resulting perceptions or behaviors can be produced simultaneously. Animals likely prioritize the production of specific neurons. One example is motor neurons, among the first-born neurons in most organisms: motor neurons are essential and required for all movement (Meng et al. 2020). The motor neuron example highlights the assumption that early-born neurons are of fundamental importance and less likely to vary compared to later-born neurons. Reinforcing this idea is work from Zebrafish, which suggests that generally, fast behaviors or those involving gross movements emerge first, as well as the neurons that allow for expressing those behaviors (Fetcho, Higashijima, and McLean 2008)(Fetcho and McLean 2010). In externally developing animals (e.g., Zebrafish), following such a developmental strategy would allow for fast escape behaviors before refined movements, likely to provide a fitness benefit. A third example comes from the evolution literature: The basal-most, wingless insect (Silverfish) has a nearly identical complement of stem cells as a winged Locust (Truman and Ball 1998). In locusts, stem cells proliferate for longer, producing thousands of extra neurons. Presumably, it is the *additional* later-born neurons that enable flight. This example illustrates how additional later-born neurons are thought to contribute to more specialized functions. Our data suggest the opposite may be true in some cases because we find more variation in early-born EL temporal cohorts: Thorax and terminus, possessing only early-born ELs, both reduce EL number (Figure 2-3). Within the abdomen in A1, neurons generated by the first (earliest) division of NB3-3 fail to express Eve (Figure 3). Also, marker gene expression among early-born ELs can vary (Figure 5). We can only speculate about why early-born temporal cohorts may be more diverse, but it could also be explained by analogy to the gene duplicate and diverge model. Adding later-born temporal cohorts may allow for the divergence of early-born temporal cohorts.

The computations performed by temporal cohorts are likely to vary along the axis.
A fundamental feature of animal body plans is axial diversity. Sensory processing circuits and motor circuits must be specialized in some manner to accommodate differences in input and

output. In theory, there are two models for how this could be done. In the first, “homogeneous model,” identical segmentally-repeating central circuits could be hooked up to different inputs (e.g., numbers and types of somatosensory neurons) and different outputs (e.g., numbers and types of motor neurons), and this could be sufficient to generate axially specialized functions. Support for such a model comes from modeling work and the evolution literature (Katz and Hale 2017)(Gjorgjieva 2013). In the second, “heterogeneous model,” central circuits are not identically repeated. Support for this comes from a recording of central pattern-generating circuits and gene expression studies showing regionalized Hox expression along the body axis across phyla (Kjaerulff and Kiehn 1996)(Cohen 1987)(Ho and O’Donovan 1993)(Stein 2018)(Weeks 1982). Still, examples of how exactly circuits are specialized are rare. Our anterograde tracing data suggest that early-born ELs, which process somatosensory stimuli, are mapped into different circuits depending on body region (Figure 6). This provides a course-grained example of how somatosensory processing circuits may be functionally specialized along the body axis.

How our findings in Drosophila may related to vertebrates.

Our work focuses on motor circuits of the Drosophila nerve cord, the analog of the vertebrate spinal cord. How might our findings in insects relate to vertebrates? There is a paucity of lineage tracing data in the spinal cord, and what evidence is available neither supports nor refutes similarities at the single stem cell lineage development level.

There are remarkable correspondences between EL neurons in arthropods and V0v neurons in vertebrates. Both express EVX homeodomain transcription factors (Heckscher et al. 2015)(Moran-Rivard et al. 2001) with the conservation of EVX gene function so high that mouse Evx can rescue the lethality of *eve* mutant Drosophila (Fujioka et al. 2003). ELs/V0v INs share other features: EL/V0v neurons come from dedicated progenitors, ELs from NB3-3, and V0vs from a ventral subset of p0 progenitors (Moran-Rivard et al. 2001)(Jay and McLean 2019)(Schmidt 1997). EL/V0vs have excitatory neurotransmitter valence (Heckscher et al. 2015) commissural morphology (Heckscher et al. 2014) and are involved in postural control (Heckscher et al. 2015)(Ruder, Takeoka, and Arber 2016). Different morphological types of ELs/V0vs are sequentially produced from one stem cell (Satou, Kimura, and Higashijima 2012)(Wang et al. 2022). Given that invertebrates and vertebrates diverged >550 million years ago (before colonizing land), the correspondences between V0v/ELs are remarkable. Correspondences could arise due to homology (presence in a common ancestor) or convergence (independent origin). Regardless, correspondences demonstrate the functional importance of EL INs and motivate the study of EL development in detail. Prior work in mouse spinal cord shows that at different axial levels, V0vs are anatomically and functionally diverse (Ruder, Takeoka, and Arber 2016). Our work on EL temporal cohorts now demonstrates correspondence in this feature of EL/V0v biology.

Conclusions

Overall, this study provides a framework for understanding how cell biological variation in stem cell lineage development impacts temporal cohort biology. Ultimately, we offer novel fundamental insight into how diverse circuits emerge from a constrained pool of stem cells in vivo.

Figure Legends

Figure 1. NB3-3 produces different numbers of ELs in different CNS regions.

(A) Illustrations of Drosophila neuroblasts. Each circle represents one neuroblast with NB3-3 in maroon. A single segment is shown in (Ai) with left and right mirror image hemisegments, each containing 30 types of neuroblasts. (Aii) The developing SEZ and nerve cord comprise a segmentally repeating set of serially homologous neuroblasts.

(B) Illustration of the Drosophila larval body with the distribution of two types of somatosensory neurons. The larval is shown in a side view, anterior to the left and dorsal up. Segments are labeled with numbers by region thorax (Th), abdomen (A), and terminus (Te). Within each segment, one symbol represents one somatosensory neuron.

(C) Illustration of how EL temporal cohorts in segment A1 are distributed into different somatosensory processing circuits. Each circle represents one cell with NB3-3 in maroon and ELs in purple. Each black box indicates a temporal cohort. Arrows represent direct synaptic connections from somatosensory neurons to ELs.

(D) Image of a wild-type Drosophila larval CNS stained with anti-Even-skipped (Eve) antibodies. Eve Lateral neurons (ELs) are located on the lateral edges of the CNS (e.g., circle in A7). The CNS is shown in dorsal view with anterior up.

(E) Quantification of EL number in the larval CNS. Each circle represents the EL count in a single hemisegment. Bold black lines show the mean. All counts were compared to those in segment A1 using an ordinary one-way ANOVA **** $p<0.0001$; ** $p<0.01$; * $p<0.05$, ns = insignificant.

(F) Illustration of the major findings of this paper. Symbols are the same as in C. Additionally, in ii, the black circular outline denotes a neuron that fails to express eve; the smaller circle represents an undifferentiated neuron; and the skull and cross bones represent cell death.

Figure 2. Neuronal cell death selectively in the terminus determines EL numbers

(A, D) Quantification of EL number in segments A7, Te1, and Te2 over development. Each circle represents the EL count in a single hemisegment. Bars show averages. (A) T-test and (D) ANOVA ns = not significant, **** = $p<0.0001$, * = <0.05. Genotypes: gray is wild type; red is *Df(3L)H99/Df(3L)H99* and organ is *ElaV>p35*.

(B-C) Images of the posterior nerve cord stained with anti-Eve in wild type and when neural cell death is blocked. Images are confocal stacks; the signal has been pseudo-colored, with warm colors indicating greater expression. Circles show ELs on the left side of the nerve cord.

Figure 3. In A1, Te1, and Te2, some NB3-3 progeny fail to express Even-skipped

(A) Illustration of an idealized lineage. The large gray circle is a neuroblast (ElaV[-]); cyan circles are neurons (ElaV[+]) of the A hemilineage (Notch ON and Hey[+]), and purple circles are neurons (ElaV[+]) of the B hemilineage (Notch OFF and Hey[-]). Green outlines show the lineage tracer expression (GFP[+]).

(B) Images of a lineage tracing experiment. The Drosophila embryonic nerve cord (stage 17) is shown in ventral view with dorsal up stained with anti-GFP(i), anti-ElaV(ii), anti-Hey(ii), and anti-Eve antibodies(iv). A small z-stack projection including all NB3-3 neurons shows the lineage in segments A6 to Te1 (circled). In this case, the lineage trace failed in the Te1 left segment. The Te2 left segment is boxed and enlarged in Bv-viii. (v-viii) A single confocal slice shows: white circle = NB3-3; cyan circle = NB3-3A neuron; solid magenta circle = NB3-3B Eve(+) neuron (an EL); dashed magenta circle = NB3-3B Eve(-) neuron. Genotype: *Eagle>G-TRACE.*

(C) Illustration of the data is shown in Bv-viii, color-coded as in Figure A, with green outlines omitted for clarity. The single Eve-expressing neuron is circled in black.

(D-E) Quantifications of the distribution of NB3-3 neuronal types. (D) NB3-3B neurons without Eve are found in segment A1, Te1, and Te2. (E) A large number of NB3-3A neurons are found in SEZ and thorax but not the abdomen or terminus. Each circle represents the cell count in a single hemisegment. Bars show averages. ANOVA **** = $p<0.0001$, *** = $p<0.001$, ** = $p<0.01$; * = <0.05. In D, comparisons are versus count in A2; in E, comparisons are versus A1. Genotype: *Eagle>G-TRACE.*

(F) Illustration of the distribution of NB3-3B neurons with and without Eve expression and NB3-3A neurons. Eve counts are taken from Figure 1.

Figure 4. The proliferation pattern of NB3-3 is distinct in each region

(A-D) Illustrations of the division patterns of NB3-3 lineage in different regions. Each circle represents one cell, and each arrow represents a cell division. Large gray circles are NB3-3; smaller gray circles are ganglion mother cells (GMCs); smaller dark gray and purple cells are NB3-3A and NB3-3B neurons, respectively. (C) An example of the ts-MARCM induction event corresponding to the clone in E' is overlaid in the boxed region. The red lightning bolt represents the heat shock that induces a recombination event. One NB3-3 descendant is labeled with GFP (green ring) and the other with RFP (red ring). Labels are inherited by subsequent descendants (e.g., multiple red rings). Maximum abdominal clone size (RFP+ and GFP+ cells) can be used to

infer heat shock time relative to NB3-3 division number, which is the X-axis in plots F-H. See methods for details.

(E) Images of an example Twin-Spot MARCM clone. Segments A1-A7 of the nerve cord are shown in dorsal view with anterior up. The boxed region in (E) is enlarged in (E'). In E' arrowheads point to labeled ELs. Genotype: *EL>ts-MARCM*.

(F) Quantification of the distribution of clones in abdominal segments. Rows represent clone type, where #:# corresponds to the number of cells labeled in each color. For example, E' shows a 1:5 clone. Columns correspond to the inferred heat shock time relative to the NB3-3 division number. Each circle indicates one or more clones were generated, with the circle size corresponding to the number of clones obtained at each time point. Clones on the diagonal from top left to bottom right correspond to stem cell recombination events, whereas clones horizontal in the 1:0 row are likely from GMC divisions.

(G-H) Quantification of the distribution of clones by time of induction and region. (G) The number of clones in each region at each heat shock time was counted and expressed as a percentage of the 234 clones in the dataset. (H) For clones at each region and time point, the "small (i.e., 1:0)" was counted and expressed as a percentage of the number of clones in that region and time. For example, the dataset contains one thoracic clone produced at relative heat shock time 2, which was 1:0 (i.e., 100%.)

(I-I"') Images and an illustration of a thoracic clone containing a small soma. The arrowhead indicates the small soma.

(J) Quantification of the distribution of clones with small soma size. Data are expressed as percentages by region. In parentheses, the total number of small soma is divided by the total number of clones in the region. "?" clone size could not be scored in the available images.

Figure 5. Early-born EL markers are found in all segments; late-born ELs are found in the SEZ and abdomen only

(A) Images of the late-born marker, 11F02 in ELs and other neurons in various segments. The nerve cord of a late-stage embryonic nerve cord is shown in a ventral view with the anterior up. In segment T2, the left ELs are circled in each image. Genotype: *11F02>nls-GFP*

(B-D) Quantification of the number of ELs per hemisegment expressing the given marker. Green = late-born marker, 11F02; orange = early-born marker, Kruppel (Kr); cyan = early-born marker, Knot (Kn). Each circle represents the cell count in a single hemisegment. The average and standard deviation are overlaid in black. ANOVA **** = $p<0.0001$, *** = $p<0.001$, ** = $p<0.01$; * = <0.05; ns = not significant with multiple comparisons to counts in A1.

Figure 6. Abdominal and terminal ELs receive input from chordotonal and bipolar dendrite somatosensory neurons, but ELs in the thorax do not.

(A) Illustration of the Trans-tango anterograde labeling system. Trans tango labels neurons expressing GAL4 in green. Neurons that receive direct synaptic input from GAL4(+) neurons are labeled in red. Here, other neurons are labeled in black, and anti-Eve (magenta) stains nuclei of EL interneurons.

(B) Image of an example Trans Tango experiment. A single image slice of a hemisegment at A4 of an L3 CNS is shown in dorsal view with anterior up, midline to the left, and scale bar of 10 microns. Arrowheads point to ELs visible in this focal plane. Solid arrows are ELs labeled by RFP, and hollow are unlabeled by RFP. (Bi) shows CHO sensory neuron termini in the CNS, (Bii) shows the membrane of neurons that form synapses with CHO sensory neurons. (Biii) shows anti-even staining. (Biv) shows the close apposition of green and red signals. (Bv) shows that ELs receive synapses from CHOs. (Bvi) is an enlargement of Bv. Genotype: *IAV-GAL4>Trans-Tango*

(C) Illustrations of somatosensory sensory neurons in Drosophila larvae. Chordotonals (CHO) are vibration sensory neurons, shown in orange, labeled by *IAV-GAL4*. Dorsal bipolar dendrtie neurons (DBD) are stretch sensors, shown in dark blue, labeled by *0165-GAL4*.

(D-E) Quantification of sensory neuron inputs onto ELs by region. Thorax includes T1-T3, and A8 represents terminus. Average and standard deviation are shown. ANOVA with ** = p>0.01. Genotypes: *IAV-GAL4>Trans-Tango; 0165-GAL4>Trans-Tango*

REFERENCES

Ahringer, J. 1996. “Posterior Patterning by the Caenorhabditis Elegans Even-Skipped Homolog Vab-7.” *Genes & Development* 10 (9): 1120–30.

Baek, M, and R S Mann. 2009. “Lineage and Birth Date Specify Motor Neuron Targeting and Dendritic Architecture in Adult Drosophila.” *The Journal of Neuroscience : The Official Journal of the Society for Neuroscience* 29 (21): 6904–16. https://doi.org/10.1523/JNEUROSCI.1585-09.2009.

Bahrampour, Shahrzad, Carolin Jonsson, and Stefan Thor. 2019. “Brain Expansion Promoted by Polycomb-Mediated Anterior Enhancement of a Neural Stem Cell Proliferation Program.” *PLoS Biology* 17 (2): e3000163. https://doi.org/10.1371/journal.pbio.3000163.

Bate, M. 1990. “The Embryonic Development of Larval Muscles in Drosophila.” *Development* 110 (3): 791–804.

Berger, Christian, S.K. Pallavi, Mohit Prasad, L.S. Shashidhara, and Gerhard M. Technau. 2005. “Cyclin E Acts under the Control of Hox-Genes as a Cell Fate Determinant in the Developing Central Nervous System.” *Cell Cycle* 4 (3): 422–25. https://doi.org/10.4161/cc.4.3.1524.

Birkholz, O, C Rickert, C Berger, R Urbach, and G M Technau. 2013. “Neuroblast Pattern and Identity in the Drosophila Tail Region and Role of Doublesex in the Survival of Sex-Specific Precursors.” *Development* 140 (8): 1830–42. https://doi.org/10.1242/dev.090043.

Birkholz, Oliver, Olaf Vef, Ana Rogulja-Ortmann, Christian Berger, and Gerhard M Technau. 2013. “Abdominal-B and Caudal Inhibit the Formation of Specific Neuroblasts in the Drosophila Tail Region.” *Development* 140 (17): 3552–64. https://doi.org/10.1242/dev.096099.

Bodmer, Rolf, and Yuh Nung Jan. 1987. “Morphological Differentiation of the Embryonic Peripheral Neurons in Drosophila.” *Roux’s Archives of Developmental Biology : The Official Organ of the EDBO* 196 (2): 69–77. https://doi.org/10.1007/BF00402027.

Bossing, T, G Udolph, C Doe, and G Technau. 1996. “The Embryonic Central Nervous System Lineages ofDrosophila Melanogaster:: I. Neuroblast Lineages Derived from the Ventral Half of the Neuroectoderm.” *Developmental Biology*, January. http://linkinghub.elsevier.com/retrieve/pii/S0012160696902407.

Cohen, Avis H. 1987. “Effects of Oscillator Frequency on Phase-Locking in the Lamprey Central Pattern Generator.” *Journal of Neuroscience Methods* 21 (2–4): 113–25. https://doi.org/10.1016/0165-0270(87)90109-9.

Dasen, Jeremy S, and Thomas M Jessell. 2009. *Chapter 6 - Hox Networks and the Origins of Motor Neuron Diversity*. *Current Topics in Developmental Biology*. Vol. 88. Current

Topics in Developmental Biology. Elsevier Inc. https://doi.org/10.1016/S0070-2153(09)88006-X.

Dasen, Jeremy S, Bonnie C Tice, Susan Brenner-Morton, and Thomas M Jessell. 2005. “A Hox Regulatory Network Establishes Motor Neuron Pool Identity and Target-Muscle Connectivity.” *Cell* 123 (3): 477–91. https://doi.org/10.1016/j.cell.2005.09.009.

Demilly, Adrien, Elena Simionato, David Ohayon, Pierre Kerner, Alain Garces, and Michel Vervoort. 2011. “Coe Genes Are Expressed in Differentiating Neurons in the Central Nervous System of Protostomes.” Edited by Franck Pichaud. *PLoS ONE* 6 (6): e21213. https://doi.org/10.1371/journal.pone.0021213.

Dixit, Richa, K Vijayraghavan, and Michael Bate. 2008. “Hox Genes and the Regulation of Movement in Drosophila.” *Developmental Neurobiology* 68 (3): 309–16. https://doi.org/10.1002/dneu.20589.

Doe, C Q. 1992. “Molecular Markers for Identified Neuroblasts and Ganglion Mother Cells in the Drosophila Central Nervous System.” *Development* 116 (4): 855–63.

Doe, Chris Q. 2017. “Temporal Patterning in the DrosophilaCNS.” *Annual Review of Cell and Developmental Biology* 33 (1): 219–40. https://doi.org/10.1146/annurev-cellbio-111315-125210.

Ellis, H. 1986. “Genetic Control of Programmed Cell Death in the Nematode C. Elegans.” *Cell* 44 (6): 817–29. https://doi.org/10.1016/0092-8674(86)90004-8.

Estacio-Gómez, Alicia, and Fernando J Díaz-Benjumea. 2014. “Roles of *Hox* Genes in the Patterning of the Central Nervous System of *Drosophila*.” *Fly* 8 (1): 26–32. https://doi.org/10.4161/fly.27424.

Evans, Cory J, John M Olson, Kathy T Ngo, Eunha Kim, Noemi E Lee, Edward Kuoy, Alexander N Patananan, et al. 2009. “G-TRACE: Rapid Gal4-Based Cell Lineage Analysis in Drosophila.” *Nature Methods* 6 (8): 603–5. https://doi.org/10.1038/nmeth.1356.

Feng, Weidong, Honorine Destain, Jayson J. Smith, and Paschalis Kratsios. 2022. “Maintenance of Neurotransmitter Identity by Hox Proteins through a Homeostatic Mechanism.” *Nature Communications* 13 (1): 6097. https://doi.org/10.1038/s41467-022-33781-0.

Feng, Weidong, Yinan Li, Pauline Dao, Jihad Aburas, Priota Islam, Benayahu Elbaz, Anna Kolarzyk, André EX Brown, and Paschalis Kratsios. 2020. “A Terminal Selector Prevents a Hox Transcriptional Switch to Safeguard Motor Neuron Identity throughout Life.” Edited by Claude Desplan and Marianne E Bronner. *eLife* 9 (January):e50065. https://doi.org/10.7554/eLife.50065.

Fetcho, Joseph R, Shin-ichi Higashijima, and David L McLean. 2008. “Zebrafish and Motor Control over the Last Decade.” *Brain Research Reviews* 57 (1): 86–93. https://doi.org/10.1016/j.brainresrev.2007.06.018.

Fetcho, Joseph R, and David L McLean. 2010. “Some Principles of Organization of Spinal Neurons Underlying Locomotion in Zebrafish and Their Implications.” *Annals of the New York Academy of Sciences* 1198 (1): 94–104. https://doi.org/10.1111/j.1749-6632.2010.05539.x.

Francius, Cédric, Audrey Harris, Vincent Rucchin, Timothy J. Hendricks, Floor J. Stam, Melissa Barber, Dorota Kurek, et al. 2013. “Identification of Multiple Subsets of Ventral

Interneurons and Differential Distribution along the Rostrocaudal Axis of the Developing Spinal Cord." *PloS One* 8 (8): e70325. https://doi.org/10.1371/journal.pone.0070325.

Fricker, Michael, Aviva M. Tolkovsky, Vilmante Borutaite, Michael Coleman, and Guy C. Brown. 2018. "Neuronal Cell Death." *Physiological Reviews* 98 (2): 813–80. https://doi.org/10.1152/physrev.00011.2017.

Fuchs, Yaron, and Hermann Steller. 2011. "Programmed Cell Death in Animal Development and Disease." *Cell* 147 (4): 742–58. https://doi.org/10.1016/j.cell.2011.10.033.

Fujioka, Miki M, Bridget C BC Lear, Matthias M Landgraf, Galina L GL Yusibova, Jian J Zhou, Kristen M KM Riley, Nipam H NH Patel, and James B JB Jaynes. 2003. "Even-Skipped, Acting as a Repressor, Regulates Axonal Projections in Drosophila." *Development* 130 (22): 5385–5400. https://doi.org/10.1242/dev.00770.

Gjorgjieva, Julijana. 2013. "Neural Circuits for Peristaltic Wave Propagation in Crawling Drosophila Larvae: Analysis and Modeling," March, 1–19. https://doi.org/10.3389/fncom.2013.00024/abstract.

Goulding, M, and E Lamar. 2000. "Neuronal Patterning: Making Stripes in the Spinal Cord." *Current Biology : CB* 10 (15): R565-8.

Gouti, Mina, and Anthony Gavalas. 2008. "Hoxb1 Controls Cell Fate Specification and Proliferative Capacity of Neural Stem and Progenitor Cells." *Stem Cells* 26 (8): 1985–97. https://doi.org/10.1634/stemcells.2008-0182.

Gunnar, Erika, Caroline Bivik, Annika Starkenberg, and Stefan Thor. 2016. "Sequoiacontrols the Type I>0 Daughter Proliferation Switch in the Developing Drosophilanervous System." *Development* 143 (20): 3774–84. https://doi.org/10.1242/dev.139998.

Hartenstein, Volker. 1993. *Atlas of Drosophila Development*. Vol. 328. Cold Spring Harbor Laboratory Press. http://books.google.com/books?id=c88TYAAACAAJ&dq=cold+spring+harbor+(author:jan+bate)&hl=&cd=3&source=gbs_api.

Heckscher, Ellie S, Shawn R Lockery, and Chris Q Doe. 2012. "Characterization of Drosophila Larval Crawling at the Level of Organism, Segment, and Somatic Body Wall Musculature." *The Journal of Neuroscience : The Official Journal of the Society for Neuroscience* 32 (36): 12460–71. https://doi.org/10.1523/JNEUROSCI.0222-12.2012.

Heckscher, Ellie S, Fuhui Long, Michael J Layden, Chein-Hui Chuang, Laurina Manning, Jourdain Richart, Joseph C Pearson, et al. 2014. "Atlas-Builder Software and the eNeuro Atlas: Resources for Developmental Biology and Neuroscience." *Development* 141 (12): 2524–32. https://doi.org/10.1242/dev.108720.

Heckscher, Ellie S, Aref Arzan Zarin, Serge Faumont, Matthew Q Clark, Laurina Manning, Akira Fushiki, Casey M Schneider-Mizell, et al. 2015. "Even-Skipped+ Interneurons Are Core Components of a Sensorimotor Circuit That Maintains Left-Right Symmetric Muscle Contraction Amplitude." *Neuron* 88 (2): 314–29.

Higashijima, S, E Shishido, M Matsuzaki, and K Saigo. 1996. "Eagle, a Member of the Steroid Receptor Gene Superfamily, Is Expressed in a Subset of Neuroblasts and Regulates the Fate of Their Putative Progeny in the Drosophila CNS." *Development* 122 (2): 527–36.

Ho, S, and MJ O'Donovan. 1993. "Regionalization and Intersegmental Coordination of Rhythm-Generating Networks in the Spinal Cord of the Chick Embryo." *The Journal of Neuroscience* 13 (4): 1354. https://doi.org/10.1523/JNEUROSCI.13-04-01354.1993.

Hobert, Oliver. 2021. “Homeobox Genes and the Specification of Neuronal Identity.” *Nature Reviews Neuroscience* 22 (10): 627–36. https://doi.org/10.1038/s41583-021-00497-x.

Homem, Catarina C. F., Marko Repic, and Jürgen A. Knoblich. 2015. “Proliferation Control in Neural Stem and Progenitor Cells.” *Nature Reviews Neuroscience* 16 (11): 647–59. https://doi.org/10.1038/nrn4021.

Jay, Michael, and David L McLean. 2019. “Reconciling the Functions of Even-Skipped Interneurons during Crawling, Swimming, and Walking.” *Current Opinion in Physiology*, Motor Control Systems, 8 (April):188–92. https://doi.org/10.1016/j.cophys.2019.02.003.

Jung, Heekyung, Julie Lacombe, Esteban O. Mazzoni, Karel F. Liem, Jonathan Grinstein, Shaun Mahony, Debnath Mukhopadhyay, et al. 2010. “Global Control of Motor Neuron Topography Mediated by the Repressive Actions of a Single Hox Gene.” *Neuron* 67 (5): 781–96. https://doi.org/10.1016/j.neuron.2010.08.008.

Jungbluth, Stefan, Esther Bell, and Andrew Lumsden. 1999. “Specification of Distinct Motor Neuron Identities by the Singular Activities of Individual *Hox* Genes.” *Development* 126 (12): 2751–58. https://doi.org/10.1242/dev.126.12.2751.

Katz, Paul S., and Melina E. Hale. 2017. “Evolution of Motor Systems.” In *Neurobiology of Motor Control*, edited by Scott L. Hooper and Ansgar Büschges, 135–76. Hoboken, NJ, USA: John Wiley & Sons, Inc. https://doi.org/10.1002/9781118873397.ch6.

Kessel, M. 1994. “Hox Genes and the Identity of Motor Neurons in the Hindbrain.” *Journal of Physiology-Paris* 88 (2): 105–9. https://doi.org/10.1016/0928-4257(94)90021-3.

Kjaerulff, Ole, and Ole Kiehn. 1996. “Distribution of Networks Generating and Coordinating Locomotor Activity in the Neonatal Rat Spinal Cord ***In Vitro*** : A Lesion Study.” *The Journal of Neuroscience* 16 (18): 5777–94. https://doi.org/10.1523/JNEUROSCI.16-18-05777.1996.

Kuan, Chia-Yi, Kevin A. Roth, Richard A. Flavell, and Pasko Rakic. 2000. “Mechanisms of Programmed Cell Death in the Developing Brain.” *Trends in Neurosciences* 23 (7): 291–97. https://doi.org/10.1016/S0166-2236(00)01581-2.

Kunz, Thomas, Karoline F Kraft, Gerhard M Technau, and Rolf Urbach. 2012. “Origin of Drosophila Mushroom Body Neuroblasts and Generation of Divergent Embryonic Lineages.” *Development* 139 (14): 2510–22. https://doi.org/10.1242/dev.077883.

Lacin, Haluk, Hui-Min Chen, Xi Long, Robert H. Singer, Tzumin Lee, and James W. Truman. 2019. “Neurotransmitter Identity Is Acquired in a Lineage-Restricted Manner in the Drosophila CNS.” *eLife* 8 (March):e43701. https://doi.org/10.7554/eLife.43701.

Lewis, E B. 1978. “A Gene Complex Controlling Segmentation in Drosophila.” *Nature* 276 (5688): 565–70.

Lints, Robyn, and Scott W. Emmons. 1999. “Patterning of Dopaminergic Neurotransmitter Identity among *Caenorhabditis Elegans* Ray Sensory Neurons by a TGFβfamily Signaling Pathway and a *Hox* Gene.” *Development* 126 (24): 5819–31. https://doi.org/10.1242/dev.126.24.5819.

Manning, Laurina, Ellie S. Heckscher, Maria D. Purice, Jourdain Roberts, Alysha L. Bennett, Jason R. Kroll, Jill L. Pollard, et al. 2012. “A Resource for Manipulating Gene Expression and Analyzing Cis-Regulatory Modules in the Drosophila CNS.” *Cell Reports* 2 (4): 1002–13. https://doi.org/10.1016/j.celrep.2012.09.009.

Marshall, Zarion D., and Ellie S. Heckscher. 2022. “The Role of Even-Skipped in Drosophila Larval Somatosensory Circuit Assembly.” *eNeuro* 9 (1): ENEURO.0403-21.2021. https://doi.org/10.1523/ENEURO.0403-21.2021.

Meng, Julia L., and Ellie S. Heckscher. 2021. “Development of Motor Circuits: From Neuronal Stem Cells and Neuronal Diversity to Motor Circuit Assembly.” *Current Topics in Developmental Biology* 142:409–42. https://doi.org/10.1016/bs.ctdb.2020.11.010.

Meng, Julia L, Zarion D Marshall, Meike Lobb-Rabe, and Ellie S Heckscher. 2019. “How Prolonged Expression of Hunchback, a Temporal Transcription Factor, Re-Wires Locomotor Circuits.” *eLife* 8 (September):505. https://doi.org/10.7554/eLife.46089.

Meng, Julia L, Yupu Wang, Robert A Carrillo, and Ellie S Heckscher. 2020. “Temporal Transcription Factors Determine Circuit Membership by Permanently Altering Motor Neuron-to-Muscle Synaptic Partnerships.” *eLife* 9 (May):e56898. https://doi.org/10.7554/eLife.56898.

Monedero Cobeta, Ignacio, Behzad Yaghmaeian Salmani, and Stefan Thor. 2017. “Anterior-Posterior Gradient in Neural Stem and Daughter Cell Proliferation Governed by Spatial and Temporal Hox Control.” *Current Biology* 27 (8): 1161–72. https://doi.org/10.1016/j.cub.2017.03.023.

Moran-Rivard, L, T Kagawa, H Saueressig, M K Gross, J Burrill, and M Goulding. 2001. “Evx1 Is a Postmitotic Determinant of V0 Interneuron Identity in the Spinal Cord.” *Neuron* 29 (2): 15–15. https://doi.org/10.1016/S0896-6273(01)00213-6.

Narayanan, C H, and V Hamburger. 1971. “Motility in Chick Embryos with Substitution of Lumbosacral by Brachial and Brachial by Lumbosacral Spinal Cord Segments.” *The Journal of Experimental Zoology* 178 (4): 415–31. https://doi.org/10.1002/jez.1401780402.

Pulver, Stefan R., Timothy G. Bayley, Adam L. Taylor, Jimena Berni, Michael Bate, and Berthold Hedwig. 2015. “Imaging Fictive Locomotor Patterns in Larval *Drosophila*.” *Journal of Neurophysiology* 114 (5): 2564–77. https://doi.org/10.1152/jn.00731.2015.

Ruder, Ludwig, Aya Takeoka, and Silvia Arber. 2016. “Long-Distance Descending Spinal Neurons Ensure Quadrupedal Locomotor Stability.” *Neuron* 92 (5): 1063–78. https://doi.org/10.1016/j.neuron.2016.10.032.

Satou, C, Y Kimura, and S i Higashijima. 2012. “Generation of Multiple Classes of V0 Neurons in Zebrafish Spinal Cord: Progenitor Heterogeneity and Temporal Control of Neuronal Diversity.” *The Journal of Neuroscience : The Official Journal of the Society for Neuroscience* 32 (5): 1771–83. https://doi.org/10.1523/JNEUROSCI.5500-11.2012.

Schmidt, H et al. 1997. “The Embryonic Central Nervous System Lineages of Drosophila Melanogaster,” September, 1–19.

Seifert, Anne. 2015. “Role of *Hox* Genes in Stem Cell Differentiation.” *World Journal of Stem Cells* 7 (3): 583. https://doi.org/10.4252/wjsc.v7.i3.583.

Stam, Floor J, Timothy J Hendricks, Jingming Zhang, Eric J Geiman, Cedric Francius, Patricia A Labosky, Frederic Clotman, and Martyn Goulding. 2012. “Renshaw Cell Interneuron Specialization Is Controlled by a Temporally Restricted Transcription Factor Program.” *Development* 139 (1): 179–90. https://doi.org/10.1242/dev.071134.

Stein, Paul S. G. 2018. “Central Pattern Generators in the Turtle Spinal Cord: Selection among the Forms of Motor Behaviors.” *Journal of Neurophysiology* 119 (2): 422–40. https://doi.org/10.1152/jn.00602.2017.

Suska, Anke, Irene Miguel-Aliaga, and Stefan Thor. 2011. “Segment-Specific Generation of Drosophila Capability Neuropeptide Neurons by Multi-Faceted Hox Cues.” *Developmental Biology* 353 (1): 72–80. https://doi.org/10.1016/j.ydbio.2011.02.015.

Technau, Gerhard M, Ana Rogulja-Ortmann, Christian Berger, Oliver Birkholz, and Christof Rickert. 2014. “Composition of a Neuromere and Its Segmental Diversification under the Control of HoxGenes in the Embryonic CNS of Drosophila.” *Journal of Neurogenetics* 28 (3–4): 171–80. https://doi.org/10.3109/01677063.2013.868459.

Truman, J W, and E E Ball. 1998. “Patterns of Embryonic Neurogenesis in a Primitive Wingless Insect, the Silverfish, Ctenolepisma Longicaudata: Comparison with Those Seen in Flying Insects.” *Development Genes and Evolution* 208 (7): 357–68.

Tsuji, Takuya, Eri Hasegawa, and Takako Isshiki. 2008. “Neuroblast Entry into Quiescence Is Regulated Intrinsically by the Combined Action of Spatial Hox Proteins and Temporal Identity Factors.” *Development* 135 (23): 3859–69. https://doi.org/10.1242/dev.025189.

Wang, Yi-wen, Chris C Wreden, Maayan Levy, Julia L Meng, Zarion D Marshall, Jason MacLean, and Ellie Heckscher. 2022. “Sequential Addition of Neuronal Stem Cell Temporal Cohorts Generates a Feed-Forward Circuit in the Drosophila Larval Nerve Cord.” *eLife* 11 (June):e79276. https://doi.org/10.7554/eLife.79276.

Weeks, J C. 1982. “Segmental Specialization of a Leech Swim-Initiating Interneuron, Cell 2051.” *The Journal of Neuroscience : The Official Journal of the Society for Neuroscience* 2 (7): 972–85.

Wreden, Christopher C, Julia L Meng, Weidong Feng, Wanhao Chi, Zarion D Marshall, and Ellie S Heckscher. 2017. “Temporal Cohorts of Lineage-Related Neurons Perform Analogous Functions in Distinct Sensorimotor Circuits.” *Current Biology : CB* 27 (10): 1521-1528.e4. https://doi.org/10.1016/j.cub.2017.04.024.

Yamaguchi, Yoshifumi, and Masayuki Miura. 2015. “Programmed Cell Death in Neurodevelopment.” *Developmental Cell* 32 (4): 478–90. https://doi.org/10.1016/j.devcel.2015.01.019.

Yu, Hung-Hsiang, Chun-Hong Chen, Lei Shi, Yaling Huang, and Tzumin Lee. 2009. “Twin-Spot MARCM to Reveal the Developmental Origin and Identity of Neurons.” *Nature Neuroscience* 12 (7): 947–53. https://doi.org/10.1038/nn.2345.

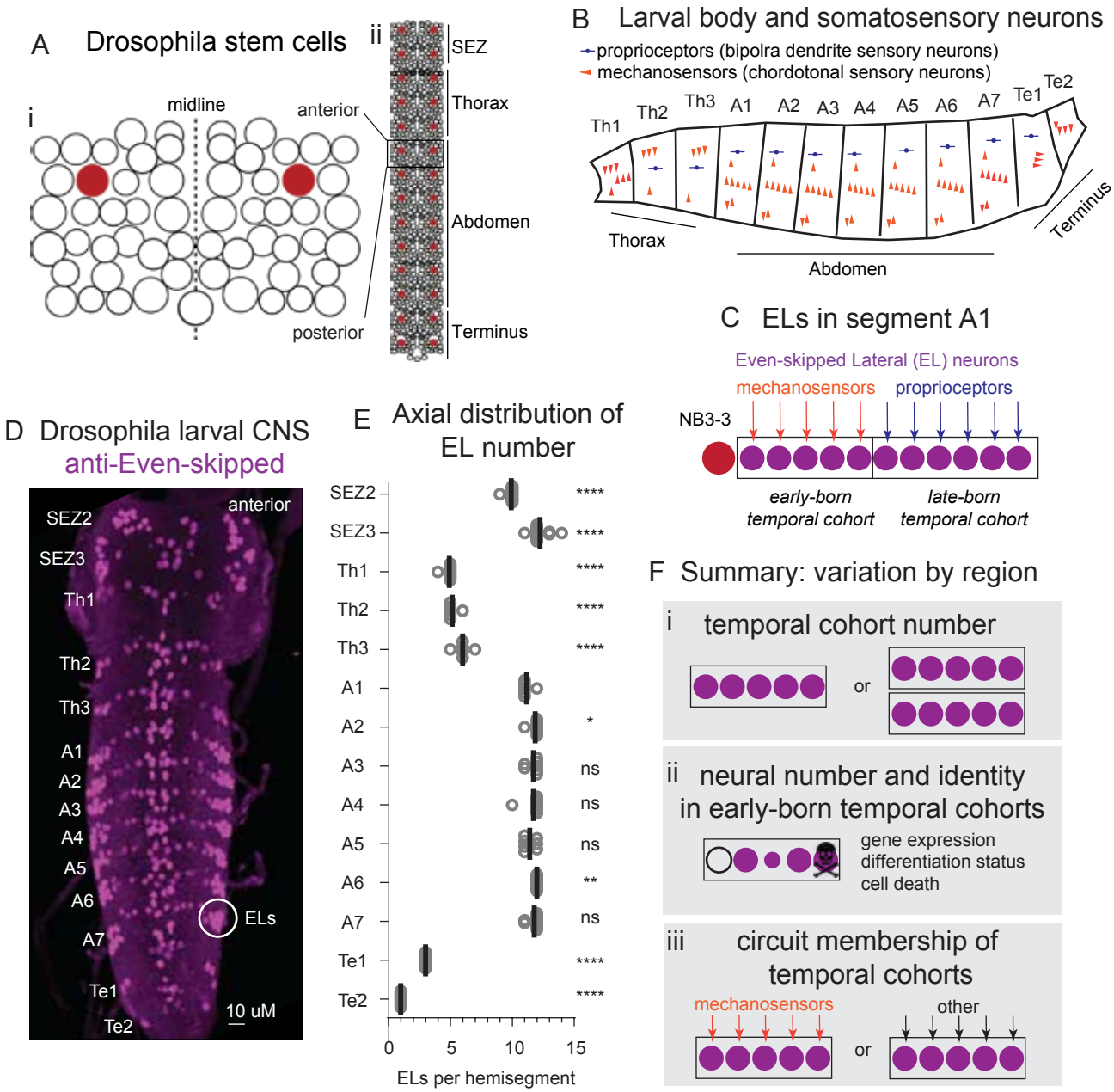
A Drosophila stem cells
i
midline
anterior
posterior
ii
SEZ
Thorax
Abdomen
Terminus
B Larval body and somatosensory neurons
proprioceptors (bipolra dendrite sensory neurons)
mechanosensors (chordotonal sensory neurons)
Th1
Th2
Th3
A1
A2
A3
A4
A5
A6
A7
Te1
Te2
Thorax
Abdomen
Terminus
C ELs in segment A1
Even-skipped Lateral (EL) neurons
mechanosensors
proprioceptors
NB3-3
early-born temporal cohort
late-born temporal cohort
D Drosophila larval CNS
anti-Even-skipped
anterior
SEZ2
SEZ3
Th1
Th2
Th3
A1
A2
A3
A4
A5
A6
A7
Te1
Te2
ELs
10 uM
E Axial distribution of EL number
SEZ2 ****
SEZ3 ****
Th1 ****
Th2 ****
Th3 ****
A1
A2 *
A3 ns
A4 ns
A5 ns
A6 **
A7 ns
Te1 ****
Te2 ****
0
5
10
15
ELs per hemisegment
F Summary: variation by region
i temporal cohort number
or
ii neural number and identity in early-born temporal cohorts
gene expression
differentiation status
cell death
iii circuit membership of temporal cohorts
mechanosensors
other
or

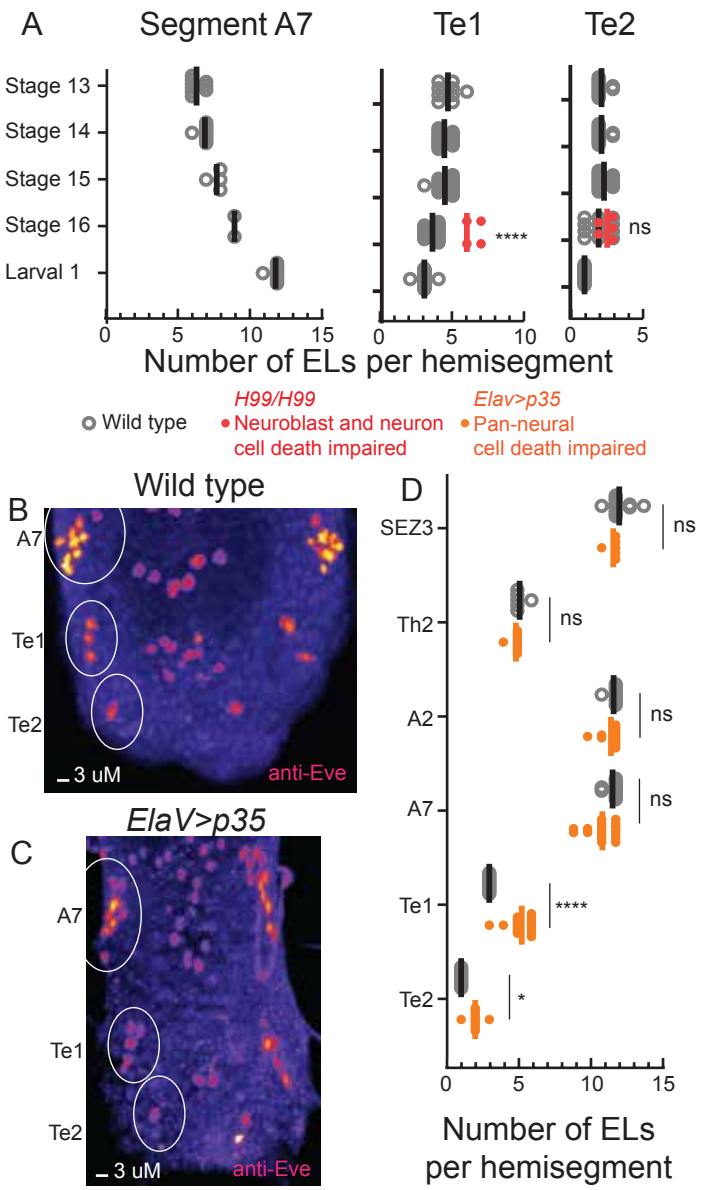
A
Segment A7
Te1
Te2
Stage 13
Stage 14
Stage 15
Stage 16
Larval 1
****
ns
0
5
10
15
Number of ELs per hemisegment
Wild type
H99/H99
Neuroblast and neuron cell death impaired
Elav>p35
Pan-neural cell death impaired
B
Wild type
A7
Te1
Te2
3 uM
anti-Eve
C
ElaV>p35
A7
Te1
Te2
3 uM
anti-Eve
D
SEZ3
Th2
A2
A7
Te1
Te2
ns
ns
ns
ns
****
*
Number of ELs per hemisegment

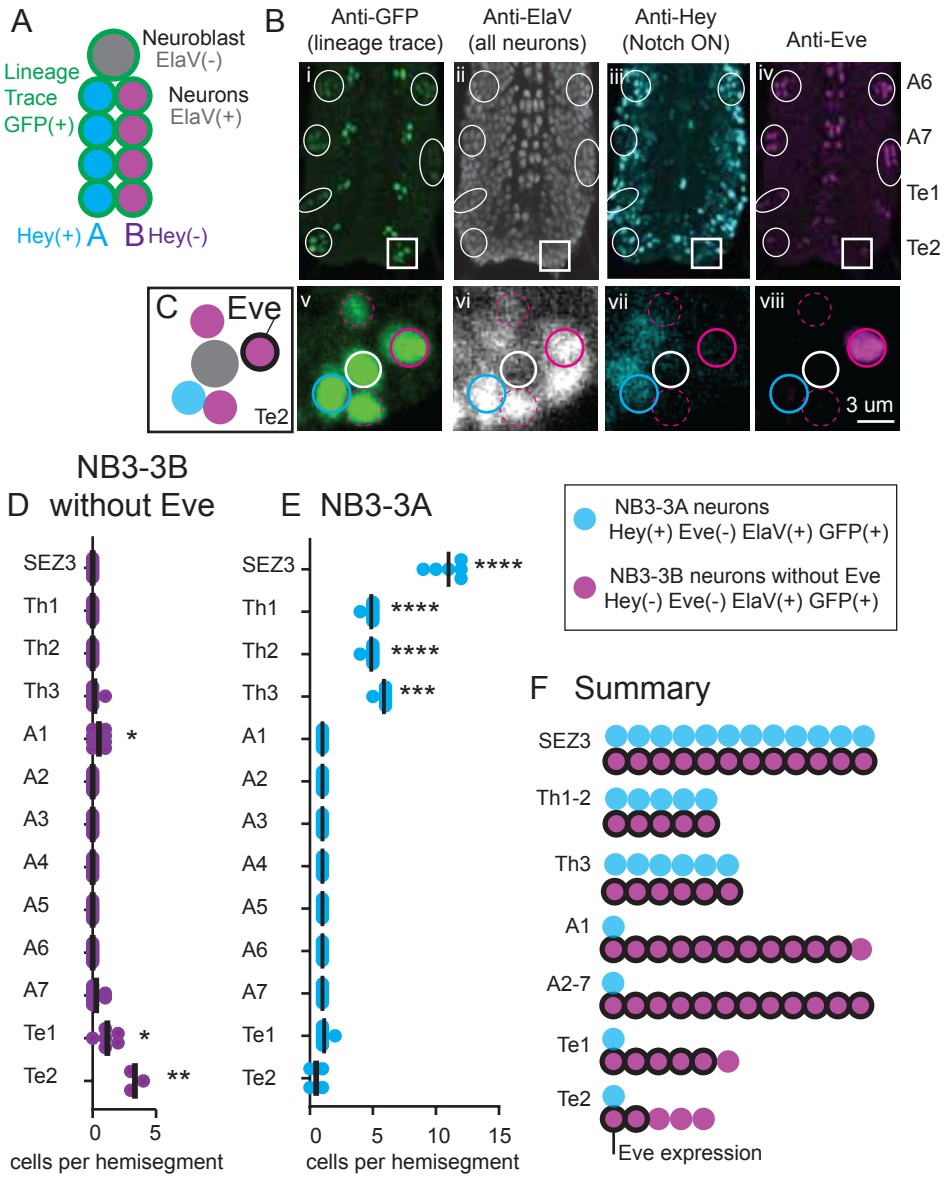
A
Neuroblast
ElaV(-)
Lineage
Trace
GFP(+)
Neurons
ElaV(+)
Hey(+) A
B Hey(-)
B
Anti-GFP
(lineage trace)
Anti-ElaV
(all neurons)
Anti-Hey
(Notch ON)
Anti-Eve
A6
A7
Te1
Te2
C
Eve
Te2
3 um
NB3-3B
D without Eve
E NB3-3A
SEZ3
Th1
Th2
Th3
A1
A2
A3
A4
A5
A6
A7
Te1
Te2
cells per hemisegment
NB3-3A neurons
Hey(+) Eve(-) ElaV(+) GFP(+)
NB3-3B neurons without Eve
Hey(-) Eve(-) ElaV(+) GFP(+)
F Summary
Th1-2
A2-7
Eve expression

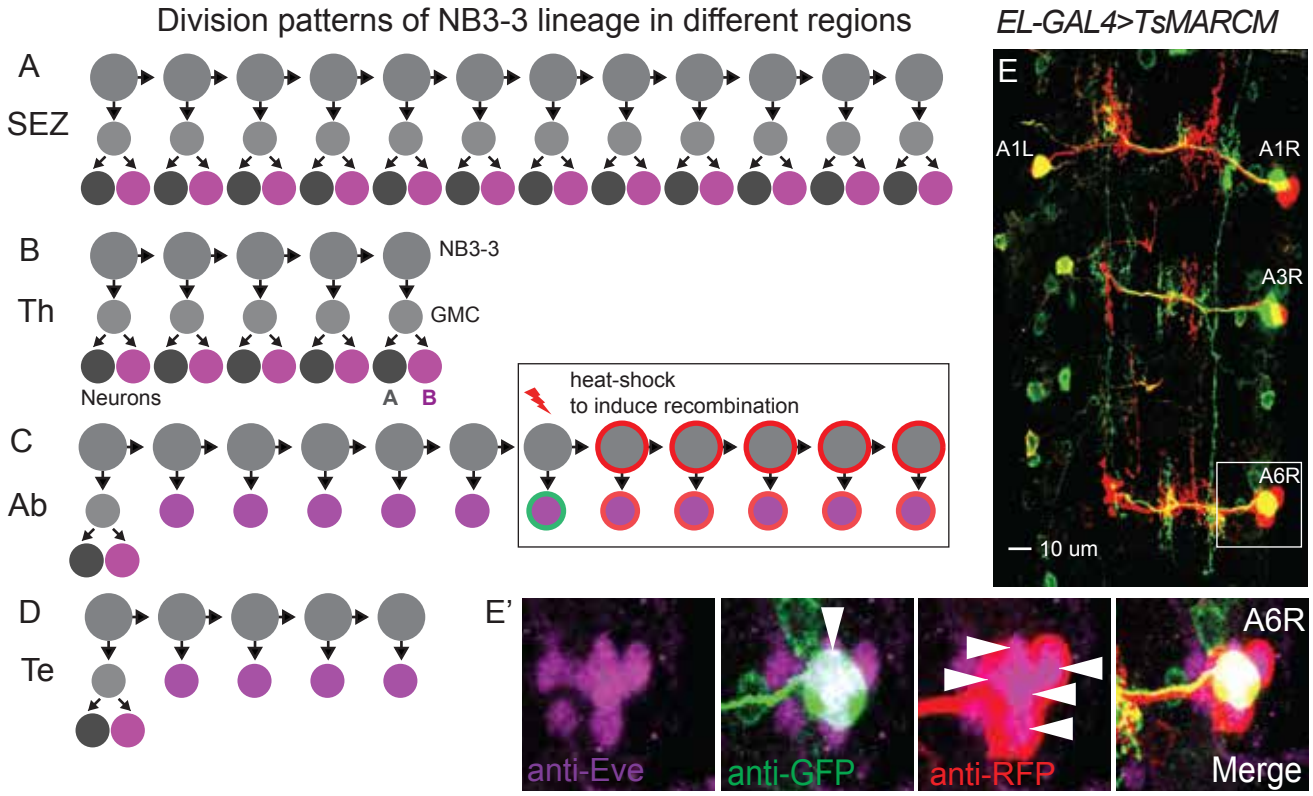

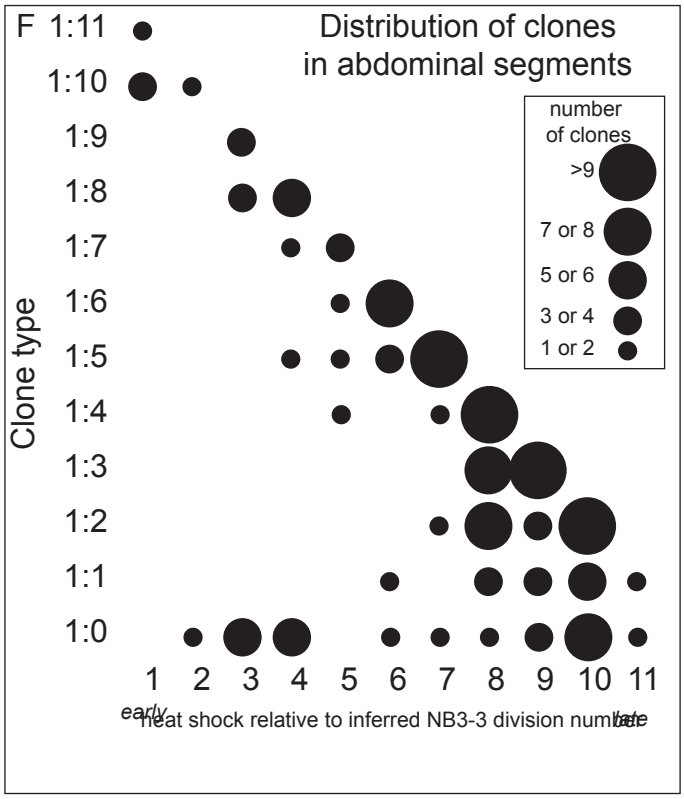

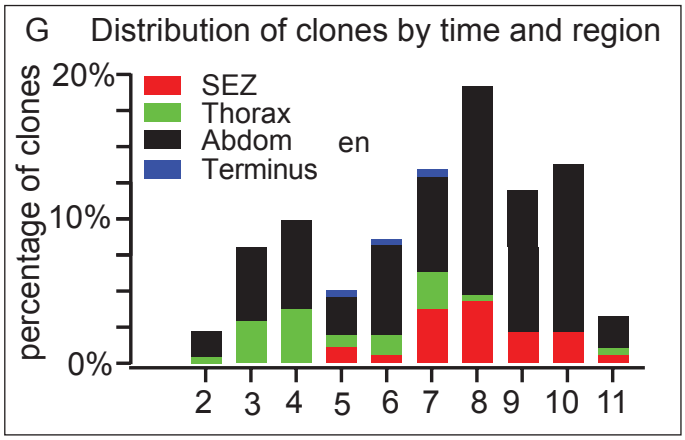

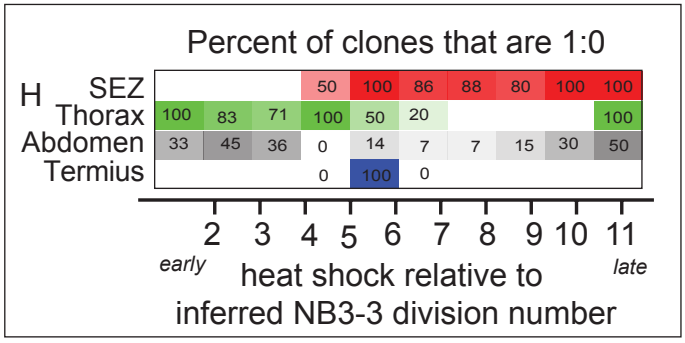

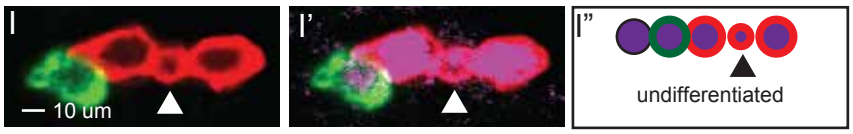

anti-GFP, anti-RFP, anti-Eve

J

SEZ	no data/35
Thorax	3/39
Abdomen	0/145
Termius	0/8

number of clones with
one small soma/total clones

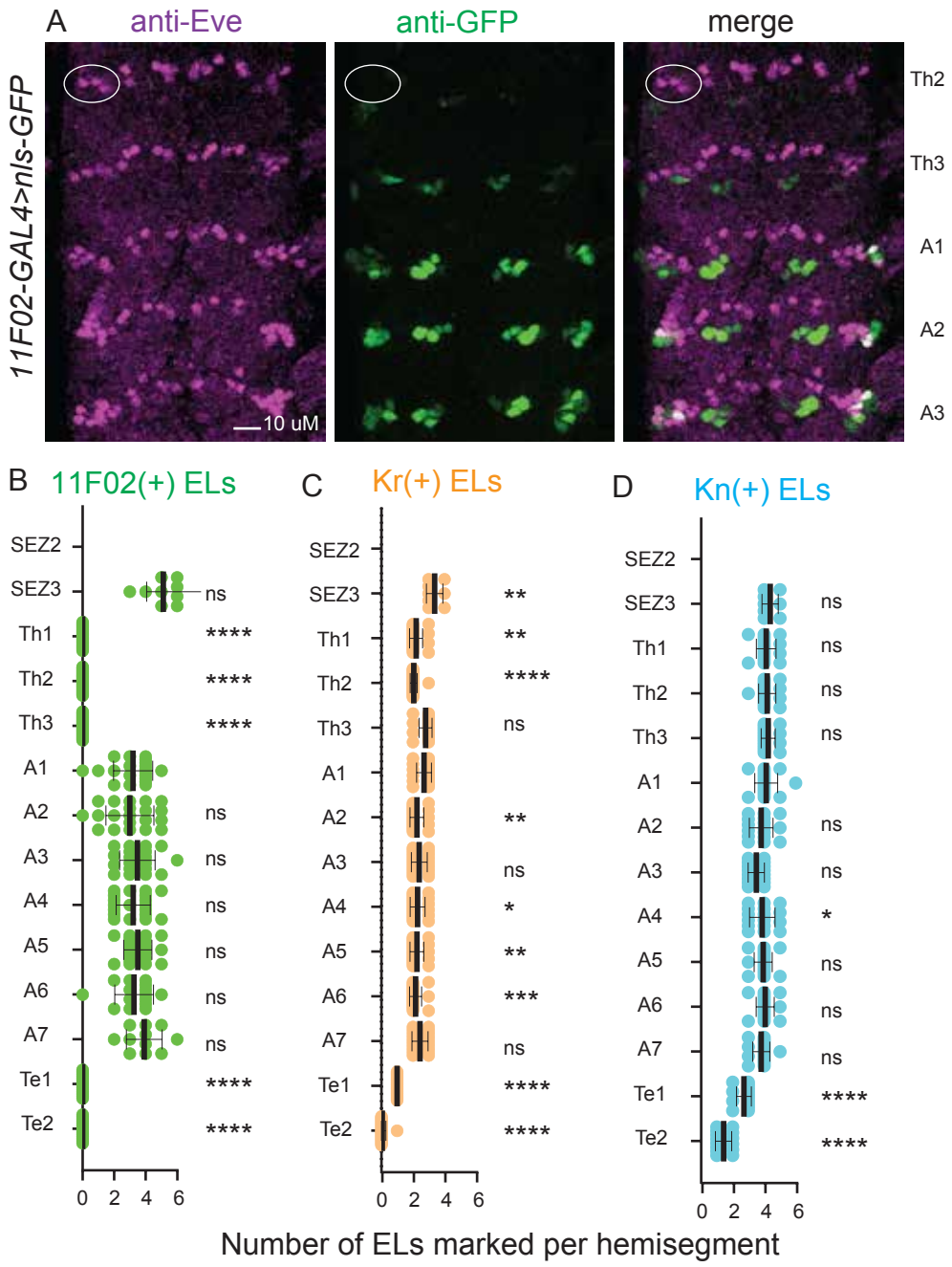
A
anti-Eve
anti-GFP
merge
11F02-GAL4>nls-GFP
10 uM
Th2
Th3
A1
A2
A3
B
11F02(+) ELs
C
Kr(+) ELs
D
Kn(+) ELs
SEZ2
SEZ3
Th1
Th2
Th3
A1
A2
A3
A4
A5
A6
A7
Te1
Te2
ns
****
**
***
*
0
2
4
6
Number of ELs marked per hemisegment

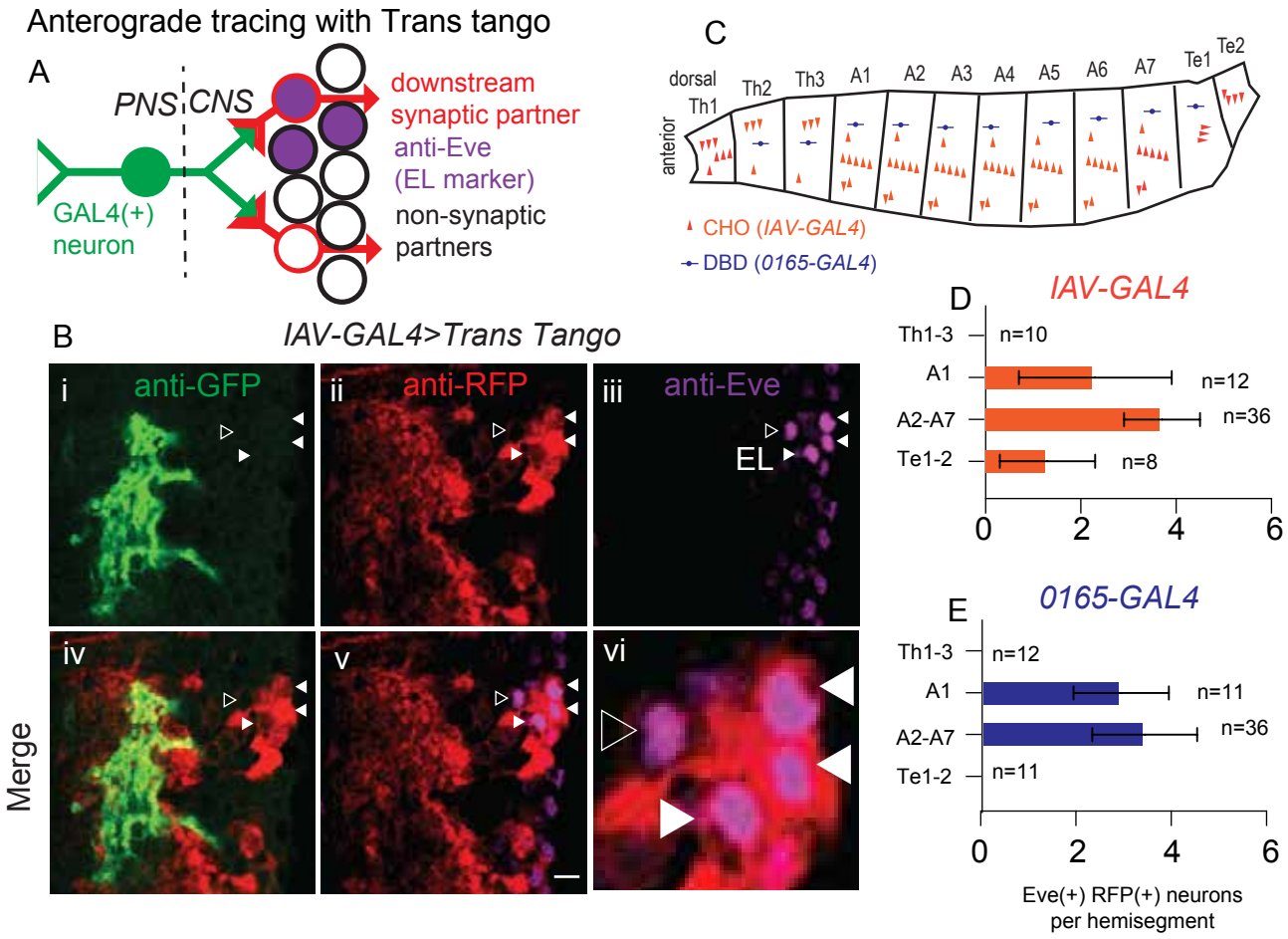
Anterograde tracing with Trans tango
A
PNS
CNS
GAL4(+)
neuron
downstream
synaptic partner
anti-Eve
(EL marker)
non-synaptic
partners
C
dorsal
anterior
Th1
Th2
Th3
A1
A2
A3
A4
A5
A6
A7
Te1
Te2
CHO (IAV-GAL4)
DBD (0165-GAL4)
B
IAV-GAL4>Trans Tango
i
anti-GFP
ii
anti-RFP
iii
anti-Eve
EL
iv
v
vi
Merge
D
IAV-GAL4
Th1-3
A1
A2-A7
Te1-2
n=10
n=12
n=36
n=8
0
2
4
6
E
0165-GAL4
Th1-3
A1
A2-A7
Te1-2
n=12
n=11
n=36
n=11
0
2
4
6
Eve(+) RFP(+) neurons
per hemisegment